analysis of the factors determining the relative strength of an oxidative fluorinator will be given in a separate paper.[43]

Acknowledgment. The authors thank Dr. Carl Schack for help, Dr. Konrad Seppelt for helpful comments on the crystal structure disorder problem, and the U.S. Army Research Office and the U.S. Air Force Phillips Laboratory for financial support of the work at Rocketdyne.

(43) Christe, K. O.; Wilson, W. W.; Dixon, D. A. To be published.

Supplementary Material Available: Table SI listing observed and calculated structure factors (2 pages). Ordering information is given on any current masthead page.

Preparation and Interconversion of Binuclear 2-Ferrazetine and Isomeric Ferrapyrrolinone Complexes

Chad A. Mirkin,[†] Kuang-Lieh Lu,[†] Thomas E. Snead,[†] Bruce A. Young,[†] Gregory L. Geoffroy,*[,†] Arnold L. Rheingold,[‡] and Brian S. Haggerty[‡]

Contribution from the Department of Chemistry, The Pennsylvania State University, University Park, Pennsylvania 16802, and Department of Chemistry, University of Delaware, Newark, Delaware 19716. *Received September 24, 1990*

Abstract: The complex $Fe_2(\mu\text{-}CH_2)(CO)_8$ reacts with the phosphine imides $R'_3P{=}NR$ (R, R' = Ph; R = Bu^t, R' = Bu^n) to form a mixture of the 3-ferra-4-pyrrolin-2-one complexes $Fe_2(\mu\text{-}CH{=}CHN(R)C\{O\})(CO)_6$ and the 2-ferrazetine complexes $Fe_2(\mu\text{-}CH{=}CHNR)(CO)_6$. The latter complexes derive from the former by loss of CO, which is accelerated by heating (50 °C, 3 h) or by adding CO-labilizing agents (halides, $[HB(s\text{-}Bu)_3]^-$). This reaction is reversed by photolysis of the 2-ferrazetine complexes under 1 atm of CO. However, when the 2-ferrazetine complexes are allowed to thermally react with CO, the isomeric 2-ferra-4-pyrrolin-3-one complexes $Fe_2(\mu\text{-}C\{O\}CH{=}CHNR)(CO)_6$ are produced instead. These latter complexes have been found to add electrophiles (HBF_4 and $[Me_3O]BF_4$) to the acyl oxygen to form the cationic complexes $[Fe_2\{\mu\text{-}C(OR){=}(CHCH{=}NBu^t)\}(CO)_8]BF_4$ (R = H, Me). The 3-ferra-4-pyrrolin-2-one complexes also react with acid (HBF_4) under 1 atm of CO to form the complexes $[Fe_2\{\mu\text{-}C(H)(CH{=}NHR)\}(CO)_8]BF_4$, which possess protonated μ_2,η^1-azallylidene ligands. The dimethylcarbene complex $Fe_2(\mu\text{-}CMe_2)(CO)_8$ also reacts with $(Bu^n)_3P{=}NBu^t$, but this reaction stops at the acyl complex $Fe_2(\mu\text{-}CMe_2)(CO)_7(C\{O\}N(Bu^t)P(Bu^n)_3)$ since this species cannot undergo the hydrogen migration needed to give entry to the ferrapyrrolinone and ferrazetine complexes. Mechanisms are proposed for these various transformations, and the following complexes have been crystallographically characterized: $Fe_2(\mu\text{-}CH{=}CHNPhC\{O\})(CO)_6$, $Fe_2(\mu\text{-}CH{=}CHNBu^t)(CO)_6$, $Fe_2(\mu\text{-}C\{O\}CH{=}CHNPh)(CO)_6$, $[Fe_2(\mu\text{-}CHCH{=}NHBu^t)(CO)_8][CF_3SO_3]$, and $[Fe_2(\mu\text{-}C\{OMe\}{=}CHCH{=}NBu^t)(CO)_8][BF_4]$.

Introduction

Phosphine imides ($R_3P{=}NR$) are common reagents in the organic chemists repertoire for deoxygenating organic carbonyl compounds to form Schiff bases, reactions that proceed by initial addition of the nucleophilic phosphine imide nitrogen atom to the electropositive carbonyl carbon, followed by elimination of phosphine oxide. In principle, carbonyl ligands attached to transition metals should also be capable of undergoing deoxygenation by phosphine imides to form isocyanide ligands, but only two examples of this reaction have been reported (eqs 1 and 2).[1-3]

$$PdCl_2 + 2PhN{=}PPh_3 + CO \rightarrow PdCl_2(C{\equiv}NPh)(Ph_3P{=}NPh) + O{=}PPh_3 \quad (1)$$

$$Ph_3P{=}NR + Fe(CO)_5 \rightarrow Fe(CO)_4(C{\equiv}NR) + Fe(CO)_3(C{\equiv}NR)_2 + Ph_3P{=}O \quad (2)$$

$$W(CO)_6 + 2Ph_3P{=}NH \rightarrow (Ph_3P{=}NH)_2W(CO)_4 + 2CO \quad (3)$$

The predominant reaction that occurs upon reaction of carbonyl complexes with phosphine imides is ligand substitution, with the phosphine imide ligand coordinating through the nitrogen atom, e.g., eq 3.[4] The first step in both processes likely involves initial formation of an acyl intermediate via nucleophilic addition of the phosphine imide nitrogen to a terminal carbonyl ligand. This intermediate can then either eliminate phosphine oxide to form an isocyanide ligand or lose another ligand as the phosphine imide migrates to the metal to yield a substituted complex (Scheme I).[5]

Scheme I

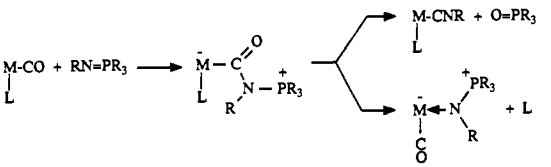

In our continuing studies of complexes containing ketene ligands,[6] we sought to determine if phosphine imides would deoxygenate a coordinated ketene ($CH_2{=}C{=}O$) to form a ketenimine ($CH_2{=}C{=}NR$) ligand. The complex $Fe_2(\mu\text{-}CH_2)(CO)_8$ (**1**) has been reported to react with nucleophiles to give products that may form via the intermediacy of a μ-ketene complex,[7] and in an attempt to trap the presumed μ-ketene intermediate, we allowed

[†] The Pennsylvania State University.
[‡] University of Delaware.

(1) (a) Kiji, J.; Matsumura, A.; Haishi, T.; Okazaki, S.; Furukawa, J. *Bull. Chem. Soc. Jpn.* **1977**, *40*, 2731.
(2) Alper, H.; Partis, R. A. *J. Organomet. Chem.* **1972**, *35*, C40.
(3) Phosphine imides are well-known to deoxygenate metal oxo complexes to form the corresponding imido compounds. See, for example: (a) Chong, A. O.; Oshima, K.; Sharpless, K. B. *J. Am. Chem. Soc.* **1977**, *99*, 3420. (b) Maatta, E. A.; Haymore, B. L.; Wentworth, R. A. D. *Inorg. Chem.* **1980**, *19*, 1055. (c) Chatt, J.; Dilworth, J. R. *J. Chem. Soc., Chem. Commun.* **1972**, 549.
(4) Bock, H.; tom Dieck, H. *Z. Naturforsch.* **1966**, *21B*, 739.
(5) Abel, E. W.; Mucklejohn, S. A. *Phosphorus Sulfur Relat. Elem.* **1981**, *9*, 235 and references therein.
(6) (a) Bassner, S. L.; Morrison, E. D.; Geoffroy, G. L.; Rheingold, A. L. *Organometallics* **1987**, *6*, 2207. (b) Morrison, E. D.; Steinmetz, G. R.; Geoffroy, G. L.; Fultz, W. C.; Rheingold, A. L. *J. Am. Chem. Soc.* **1986**, *106*, 4783.
(7) (a) Denise, B.; Navarre, D.; Rudler, H. *J. Organomet. Chem.* **1987**, *326*, C83. (b) Navarre, D.; Rudler, H.; Daran, J. C. *J. Organomet. Chem.* **1986**, *314*, C34. (c) Röper, M.; Strutz, H.; Keim, W. *J. Organomet. Chem.* **1981**, *219*, C5.

0002-7863/91/1513-3800$02.50/0 © 1991 American Chemical Society

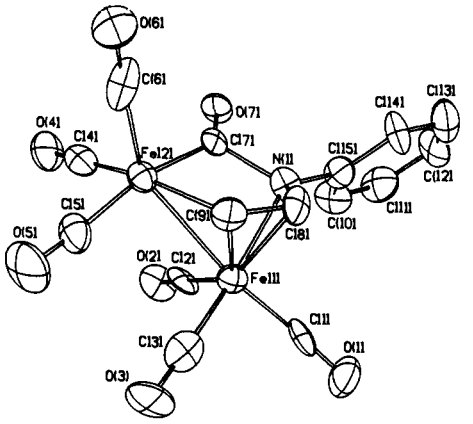

Figure 1. ORTEP drawing of $Fe_2(\mu\text{-}CH{=}CHNPhC\{O\})(CO)_6$ (**2b**). Thermal ellipsoids are drawn at 40% probability.

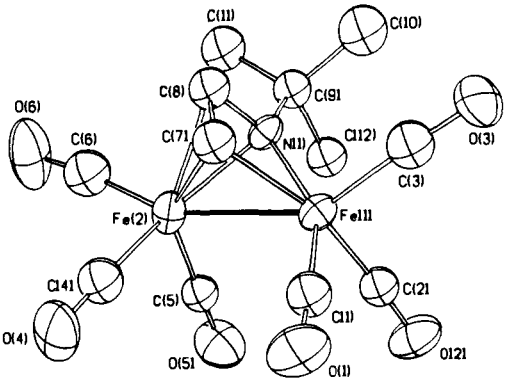

Figure 2. ORTEP drawing of one of two chemically similar but crystallographically independent molecules of $Fe_2(\mu\text{-}CH{=}CHNBu^t)(CO)_6$ (**3a**). Thermal ellipsoids are drawn at 40% probability.

complex **1** to react with the phosphine imides $(Bu^n)_3P{=}NBu^t$ and $Ph_3P{=}NPh$. However, as reported in detail herein and earlier communicated,[8] these reactions did not yield detectable ketenimine complexes but instead gave an unprecedented series of transformations yielding binuclear ferrapyrrolinone and ferrazetine compounds. These complexes have been spectroscopically and crystallographically characterized, and aspects of their reactivity have been examined. Particularly interesting is the ability of the ferrazetine complex to undergo reversible carbonylation to form isomeric ferrapyrrolinone complexes that differ in the site of CO incorporation, depending upon whether photochemical or thermal conditions are used. Also intriguing is the rearrangement that occurs to form a protonated azallylidene ligand when the ferrazetine complex is treated with HBF_4.

Results

Reaction of $Fe_2(\mu\text{-}CH_2)(CO)_8$ with Phosphine Imides. Under 1 atm of CO, the complex $Fe_2(\mu\text{-}CH_2)(CO)_8$ (**1**) rapidly reacted with the phosphine imides $(Bu^n)_3P{=}NBu^t$ and $Ph_3P{=}NPh$ to form a mixture of the 3-ferra-4-pyrrolin-2-one **2a,b** and 2,3-ferrazetine **3a,b** complexes shown in eq 4. The names of these

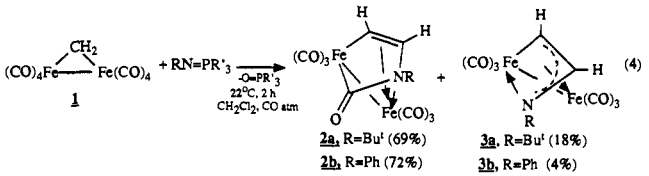

species derive from the corresponding organic ring systems drawn below. They were isolated as microcrystalline solids and have been spectroscopically characterized, with complexes **2b** and **3a** further defined by X-ray diffraction studies (Figures 1 and 2). The predominant products of reaction 4 were the ferrapyrrolinone complexes **2a** and **2b**. The spectroscopic data for these species

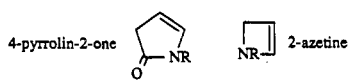

(see Experimental Section) are similar and fully consistent with the crystal structure of **2b**. Also formed in reaction 4 are the 2,3-ferrazetine complexes **3a** and **3b**. As shown below, these derive from the ferrapyrrolinone complexes **2a,b** by loss of CO, and such reaction may account for their formation in reaction 4. Indeed, the product ratio shifts significantly in the direction of **3** when the reaction is conducted in the absence of a CO atmosphere. Complexes **3a,b** are spectroscopically similar (see Experimental Section), and their data are consistent with the structure determined for **3a** (Figure 2).

To our knowledge, the 3-ferra-4-pyrrolin-2-one complexes **2a,b** are the first metallacycles to have this specific structure, although the isomeric 2-metalla-3-pyrrolin-4-one complexes I–IV have been prepared by other means.[9] Note that the arrangement of the ring carbonyls and the imido groups in these compounds are different from that of **2a,b**. A diiron analogue of **2a,b** having a sulfur atom in place of the nitrogen atom is also known.[10] Examples of

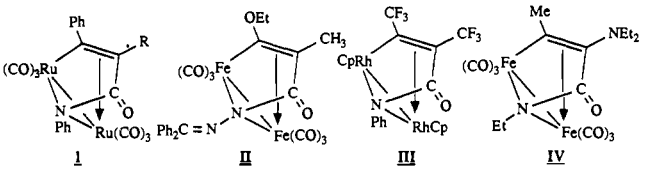

2,3-ferrazetine complexes analogous to **3a,b** have been previously prepared in low yield by the simultaneous addition of azirines and alkynes to $Fe_2(CO)_9$ (eq 5), and the specific derivative given in the equation was crystallographically characterized.[11] Diiron and dicobalt analogues of **3a,b** having a phosphorus atom in place of the nitrogen atom are also known, as are sulfur and oxygen analogues.[12]

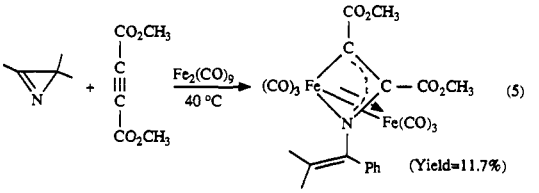

A minor product (**4a**) was isolated in low yield (4%) from the reaction of complex **1** with $Bu^tN{=}P(Bu^n)_3$. Spectroscopic data indicate it to be a derivative of **2a** having a $Bu^tN{\equiv}C$ ligand substituted for one of the CO ligands. However, the spectroscopic data do not indicate to which iron atom the isocyanide ligand is bound. The mass spectrum of **4a** showed a parent ion at m/z

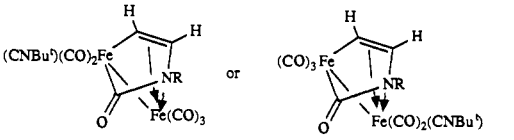

4a

(8) Mirkin, C. A.; Lu, K. L.; Geoffroy, G. L.; Rheingold, A. L.; Staley, D. *J. Am. Chem. Soc.* **1989**, *111*, 7279.

(9) (a) Han, S. H.; Geoffroy, G. L.; Rheingold, A. L. *Organometallics* **1987**, *6*, 2380. (b) Nuel, D.; Dahan, F.; Mathieu, R. *Organometallics* **1986**, *5*, 1278. (c) Dickson, R. S.; Nesbit, R. J.; Pateras, H.; Baimbridge, W.; Patrick, J. M.; White, A. H. *Organometallics* **1985**, *4*, 2128. (d) Crocq, V.; Daran, J. C.; Jeannin, Y. *J. Organomet. Chem.* **1989**, *373*, 85. (e) For mononuclear metallapyrrolinone complexes see: Hoberg, H.; Hernandez, E.; Guhl, D. *J. Organomet. Chem.* **1988**, *339*, 213 and references therein.

(10) Fässler, T.; Huttner, G.; Günauer, D.; Fiedler, S.; Eber, B. *J. Organomet. Chem.* **1990**, *381*, 409.

(11) Nakamura, Y.; Bachmann, K.; Heimgartner, H.; Schmid, H.; Daly, J. J. *Helv. Chim. Acta* **1978**, *61*, 589.

(12) (a) Lang, H.; Zsolnai, L.; Huttner, G. *Chem. Ber.* **1985**, *118*, 4426. (b) Werner, H.; Zolk, R. *Chem. Ber.* **1987**, *120*, 1003. (c) Schrauzer, G. N.; Kirsch, H. *J. Am. Chem. Soc.* **1973**, *95*, 2501. (d) Yanez, R.; Ros, J.; Solans, X.; Font-Bardia, M.; Mathieu, R. *J. Organomet. Chem.* **1990**, *388*, 169.

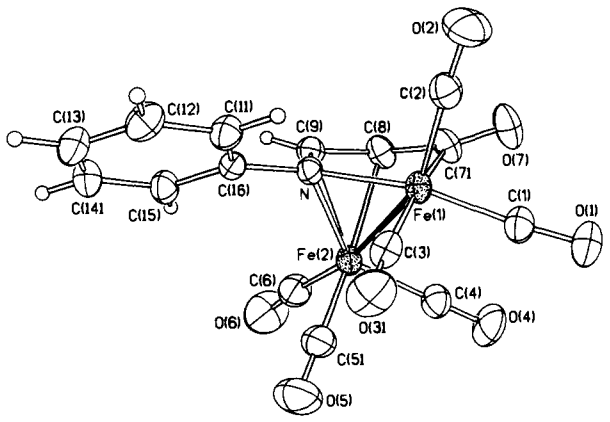

Figure 3. ORTEP drawing of $Fe_2(\mu\text{-}C\{O\}CH{=}CHNPh)(CO)_6$ (**5b**). Thermal ellipsoids are drawn at 40% probability.

Scheme II

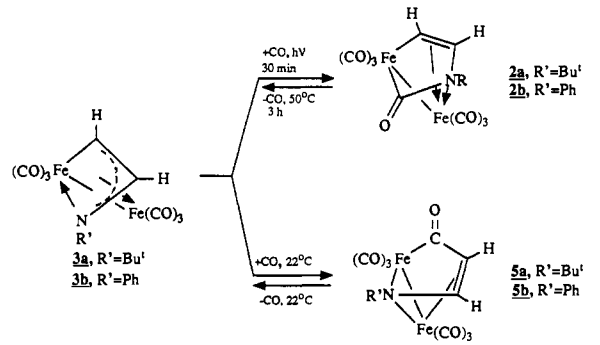

460 followed by peaks corresponding to the successive loss of five carbonyls, consistent with the indicated formulation. Its ^1H and ^{13}C NMR spectra are similar to that of the 3-ferra-4-pyrrolin-2-one complex **2a**, implying the presence of a similar ring system. Particularly significant in the IR spectrum of **4a** is a band at 2164 cm^{-1} assigned to the isocyanide ligand along with a 1650 cm^{-1} acyl vibration and a series of metal carbonyl bands. An apparently similar compound (**4b**) formed in trace quantities in the reaction of **1** with $Ph_3P{=}NPh$, but its low yield precluded full characterization.

Reversible Carbonylation of the 2,3-Ferrazetine Complexes To Form Isomeric Ferrapyrrolinone Complexes. As illustrated in Scheme II, the ferrazetine complexes **3a,b** have been found to undergo reversible carbonylation to give isomeric ferrapyrrolinone complexes, depending upon whether thermal or photochemical conditions are used. Under photochemical conditions in the presence of 1 atm of CO, the 3-ferra-4-pyrrolin-2-one complexes **2a,b** were formed in near quantitative yield. However, when complexes **3a,b** were stirred at room temperature under 1 atm of CO, carbonylation occurred at the other end of the metallacycle to give the new 2-ferra-4-pyrrolin-3-one complexes **5a,b** but with no trace of **2a** or **2b**. For complex **3b**, this latter reaction was rapid (1 h) and **5b** was isolated in 72% yield by slow evaporation of solvent under a CO atmosphere. However, with complex **3a**, ^1H NMR analysis showed formation of an equilibrium mixture of **5a** (18%) and **3a** (82%) and we were unable to isolate **5a** because of its facile conversion back to **3a** when the CO atm was removed. Similarly, complex **5b** reformed **3b** when solutions were stirred under a N_2 atmosphere. Complex **5b** was fully characterized by a crystallographic study (Figure 3), and its spectroscopic data (see Experimental Section) are consistent with the determined structure.

As illustrated in Scheme II, the 3-ferra-4-pyrrolin-2-one complexes **2a,b** lost CO to form the ferrazetine complexes **3a,b** when solutions were heated to 50 °C for 3 h under a N_2 purge. However, at 22 °C, CO loss was slow and required several days for complete reaction, although the addition of halides and hydride donors markedly accelerated the reaction. This is illustrated by the half-lives given in Table I for the conversion of **2a,b** into **3a,b**

Table I. Half-Lives for the Deinsertion of CO from Complex **2** in THF at 22 °C

promoter (0.1 equiv)	$t_{1/2}$ R = Ph	$t_{1/2}$ R = Bu^t
no promoter	18 h	30 h
$K[B(s\text{-}Bu)_3H]$	<1 min	<1 min
[PPN]Cl	10 min	4 h
[PPN]Br	30 min	12 h
[PPN]I	9 h	19 h

when the reaction was conducted in the presence of [PPN]X ($PPN^+{=}(PPh_3)_2N^+$; X = Cl, Br, I) and $K[BH(s\text{-}Bu)_3]$. These reactions were carried out by predissolving 0.1 equiv of the [PPN]X promoter in 1 mL of CH_2Cl_2 followed by addition of this solution to 30 mL of a 0.002 M THF solution of complex **2a,b** or by adding 0.1 equiv of a THF solution of $K[BH(s\text{-}Bu)_3]$ directly to solutions of **2a,b**. The data given in Table I show the order of promoting ability to be $[BH(s\text{-}Bu)_3]^- \gg Cl^- > Br^- > I^-$, similar to the ordering observed for the anion-promoted ligand substitution reactions of $Ru_3(CO)_{12}$.[13] In the latter chemistry, the promoter is believed to enhance the rate of dissociation of a CO ligand from one of the metal centers, and it has been suggested that this occurs by addition of the promoter to a carbonyl ligand to form an acyl ligand.[13c] In the case of **2a,b** a similar promoted CO dissociation would open a coordination site for the deinsertion of CO to occur from the metallacycle.

The data of Table I show that the deinsertion process is generally slower for **2a** (R = Bu^t) than it is for **2b** (R = Ph). This may be due to the electron-donating *tert*-butyl group, giving an increased contribution of resonance form B, which would have a stronger carbon–nitrogen bond and a decreased tendency of this bond to break in the deinsertion step. Resonance forms like these are important for organic amides where it is known that the stretching frequency of the carbonyl group decreases as electron-donating groups are added to the amide nitrogen.[14]

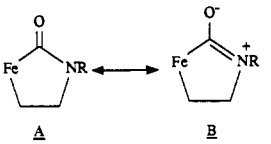

A B

With the characterization of complexes **5a,b**, three different isomers of ferrapyrrolinone complexes are now known, as illustrated by the drawings of the metallacycles in C–E below. Compounds with structure E had been prepared earlier,[9] whereas complexes **2a,b** and **5a,b** are the first examples of metallacycles C and D, respectively. As illustrated above, metallacycles C and D can be interconverted by CO insertion/deinsertion sequences, but metallacycle E cannot be accessed from these compounds.

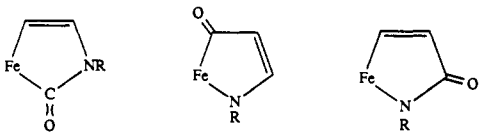

C (2a,b) D (5a,b) E

Protonation of the 3-Ferra-4-pyrrolin-2-one Complexes To Form Complexes with Protonated μ_2,η^1-Azallylidene Ligands. Protonation of the ferrapyrrolinone complexes **2a,b** with HBF_4 or CF_3SO_3H induced rearrangement and incorporation of an additional CO ligand to form complexes **6a,b**, which possess protonated azallylidene ligands (eq 6). The yields of these reactions were optimized when conducted under a CO atmosphere, although the same products formed in modest yields even when run under an N_2 atmosphere. Complexes **6a,b** were isolated as microcrys-

(13) (a) Lavigne, G.; Kaesz, H. D. *J. Am. Chem. Soc.* **1984**, *106*, 4647. (b) Lavigne, G.; Lugan, N.; Bonnet, J. *Inorg. Chem.* **1987**, *26*, 2345. (c) Lavigne, G.; Kaesz, H. D. In *Metal Clusters in Catalysis*; Knozinger, H., Gates, B. C., Guczi, L., Eds.; Elsevier: Amsterdam, 1986; pp 68–69.

(14) Zabieky, J., Ed. *The Chemistry of Amides*; Wiley-Interscience: London, 1970.

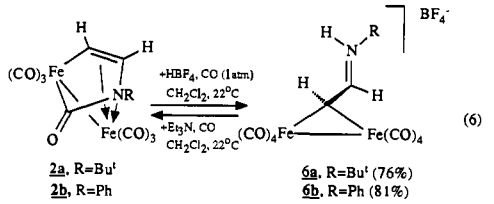

(6)

talline solids and spectroscopically defined. The $CF_3SO_3^-$ salt of complex **6a**, prepared by protonation of **2a** with CF_3SO_3H, was also crystallographically characterized, and an ORTEP drawing is shown in Figure 4. The spectroscopic data for **6a** and **6b** (see Experimental Section) are similar and fully consistent with the determined structure. Noteworthy among the spectroscopic data are the ^{13}C NMR carbene carbon resonances at δ 89.4 for **6a** and δ 89.9 for **6b**, which are further upfield than any of the resonances reported for the carbene ligands for other members of the $Fe_2(CO)_8(\mu\text{-}CRR')$ family.[15] Significantly, complexes **6a,b** rapidly and quantitatively reformed the ferrapyrrolinone complexes **2a,b** when deprotonated with excess base (Et_3N or phosphine imide; eq 6). This latter reaction likely involves deprotonation followed by attack of the phosphine imide nitrogen on a CO ligand to form the ferrapyrrolinone ring, concomitant with CO loss from the metal framework (see Discussion).

Alkylation and Protonation of the 2-Ferra-4-pyrrolin-3-one Complex 5a To Form Cationic 2-Ferrapyrrole Complexes. As illustrated in Scheme III, addition of $[Me_3O]BF_4$ to the **3a/5a** equilibrium mixture led to the high-yield formation of the 2-ferrapyrrole complex **7a**, which was isolated as a microcrystalline solid. Complex **7a** was crystallographically characterized (see Figure 5), and its spectroscopic data are consistent with the determined structure (see Experimental Section). The **3a/5a** equilibrium mixture also undergoes protonation with HBF_4 to yield mainly the hydroxy-substituted 2-ferrapyrrole complex **8a** shown in Scheme III. Also formed in low yield in the protonation reaction is a second compound **9a**; Scheme III). The inseparable mixture was isolated in modest yield as a microcrystalline solid. The ^1H and ^{13}C NMR data given in the Experimental Section for **8a** are nearly identical with those of **7a**, consistent with its indicated formulation. For example, its ^{13}C NMR spectrum showed a resonance at δ 228.4 for the Fe*C*{OH}CH carbon and resonances at δ 126.3 (dd, $^1J_{CH}$ = 190.4 Hz, $^2J_{CH}$ = 7.3 Hz) and 87.0 (dd, $^1J_{CH}$ = 179.4 Hz, $^2J_{CH}$ = 9.8 Hz) for the remaining ring carbons. In the ^1H NMR spectrum, a broad resonance at δ 10.17 was assigned to the OH proton, doublets at δ 7.37 and 6.53 (J_{HH} = 2.4 Hz) were attributed to the ring protons, and a singlet at δ 1.32 was assigned to the *tert*-butyl protons. The spectroscopic data for compound **9a** (see Experimental Section) indicate its formulation as a BF_3 adduct of **5a** (Scheme III). It is noteworthy that exposure of the **8a/9a** mixture to weak bases, even tetrahydrofuran, resulted in deprotonation/BF_3 abstraction, loss of CO, and regeneration of complex **3a**. Neutral diiron complexes structurally related to **7a** and **8a** having a sulfur atom in place of the nitrogen atom are known.[10]

Reaction of $Fe_2(\mu\text{-}CMe_2)(CO)_8$ with $(Bu^n)_3P{=}NBu^t$ To Form $Fe_2(\mu\text{-}CMe_2)(CO)_7\{C(O)N(Bu^t)P(Bu^n)_3\}$. The μ-CMe_2 analogue of complex **1** was also observed to react with $(Bu^n)_3P{=}NBu^t$ but in this case to form the zwitterionic complex **11** (eq 7). This species was isolated as a dark red oil and spectroscopically characterized. Its ^1H NMR spectrum showed, in addition to characteristic *n*-butyl resonances, singlets at δ 1.35 and 2.90 in a 3:2 intensity ratio respectively assigned to the *tert*-butyl and the methyl hydrogens. The ^{13}C NMR spectrum of **11** showed

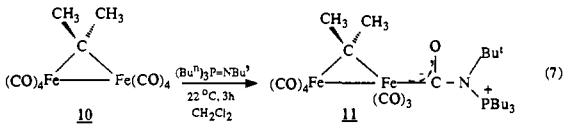

(7)

(15) Sumner, C. E., Jr.; Collier, J. A.; Pettit, R. *Organometallics* **1982**, *1*, 1350.

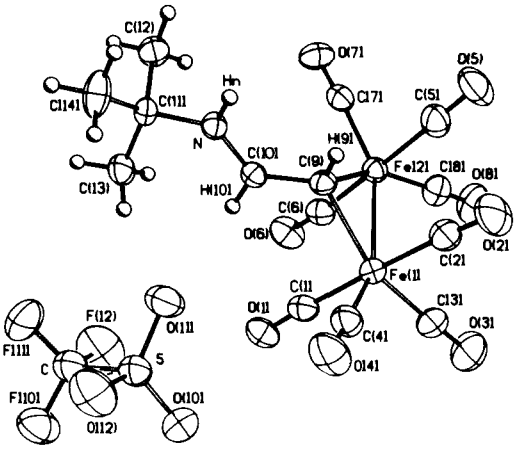

Figure 4. ORTEP drawing of $[Fe_2(\mu\text{-}CHCH{=}NHBu^t)(CO)_8][CF_3SO_3]$ (**6a'**). Thermal ellipsoids are drawn at 40% probability.

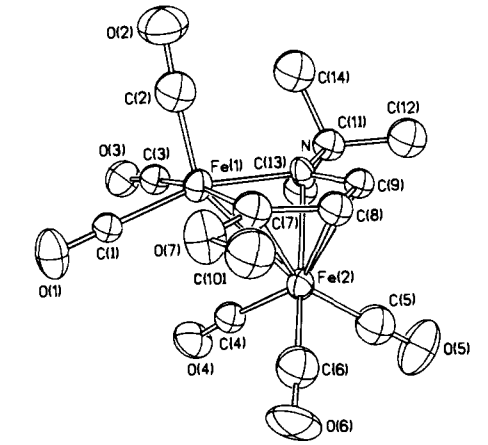

Figure 5. ORTEP drawing of $[Fe_2(\mu\text{-}C\{OMe\}CHCHNBu^t)(CO)_8][BF_4]$ (**7a**). Thermal ellipods are drawn at 40% probability.

Scheme III

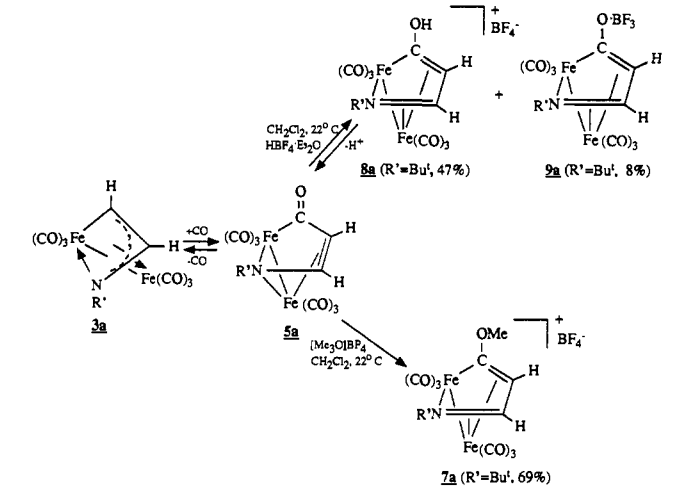

a resonance at δ 231.7 assigned to the acyl carbon, a single resonance at δ 206.3 attributed to the rapidly exchanging carbonyl ligands, and a resonance at δ 173.4 assigned to the carbene carbon, along with *n*-butyl and *tert*-butyl carbon resonances. The ^{31}P NMR resonance at δ 53.7 observed for **11** is in the typical range for quaternary phosphorus atoms (e.g., $[(Bu^n)_3PNHBu^t]Cl$, δ 51.9).[16] The IR spectrum of **11** showed a ν_{CO} stretch at 1752 cm^{-1} assigned to the acyl ligand as well as characteristic metal carbonyl vibrations.

Crystal and Molecular Structures of Complexes 2b, 3a, 5b, and 7a. ORTEP drawings of these four complexes are given in Figures

(16) Synthesized in these laboratories by the method of ref 3a.

Table II. Crystal, Data Collection, and Refinement Parameters for $Fe_2(\mu\text{-CH=CHNPhC\{O\}})(CO)_6$ (**2b**), $Fe_2(\mu\text{-CH=CHNBu}^t)(CO)_6$ (**3a**), and $Fe_2(\mu\text{-C\{O\}CH=CHNPh})(CO)_6$ (**5b**)

	2b	**3a**	**5b**
	Crystal Parameters		
formula	$C_{15}H_7Fe_2NO_7$	$C_{12}H_{11}Fe_2NO_6$	$C_{15}H_7Fe_2NO_7$
fw	424.90	376.90	424.90
crystal system	orthorhombic	monoclinic	monoclinic
space group	$Pbc2_1$ (nonstandard $Pca2_1$)	$P2_1/n$	$P2_1/n$
a, Å	20.525 (8)	10.181 (3)	8.925 (4)
b, Å	13.053 (5)	9.651 (2)	12.675 (6)
c, Å	12.735 (4)	32.25 (1)	14.597 (6)
β, deg		93.37 (3)	98.36 (3)
V, Å^3	3411 (2)	3163 (2)	1633 (1)
Z	8	8	4
μ (Mo Kα), cm^{-1}	17.4	18.55	18.11
D_{calc}, g cm^{-3}	1.655	1.583	1.728
color	orange	orange	red-brown
size, mm	0.24 × 0.31 × 0.28	0.31 × 0.25 × 0.20	0.24 × 0.31 ×0.34
temp, K	293	296	296
	Data Collection		
diffractometer		Nicolet R3m	
monochromator		graphite	
scan method		Wyckoff	
radiation		Mo Kα	
wavelength, Å		0.71073	
scan lim, deg	$4 \le 2 \le 45$	$4 \le 2\theta \le 42$	$4 \le 2\theta \le 55$
data collected	+23, +15, +14	±11, +10, +33	±12, +17, +20
reflectn collected	2541	3816	5346
indepent reflectn	2340	3395	5127
R_{int}, %	n.a.	5.20	2.60
obsvd reflectn	1839	1688	3337
	$F_o \ge 5\sigma(F_o)$	$F_o \ge 5\sigma(F_o)$	$F_o \ge 5\sigma(F_o)$
	Refinement		
$R(f)$, %	5.59	8.29	3.92
$R(wf)$, %	5.38	7.33	4.29
$\Delta(\rho)$, e Å^{-3}	0.62	0.54	0.40
Δ/σ_{max}	0.023	0.030	0.015
N_o/N_v	4.31	7.46	15.59
GOF	1.350	1.303	1.124

1–3 and 5, and pertinent crystallographic details are set out in Tables II–XI. Each of these complexes possesses two $Fe(CO)_3$ units joined by an Fe–Fe bond and bridged by an organic ligand. The Fe–Fe bond distances in the four compounds are similar (**3a**, 2.476 (3) Å; **5b**, 2.557 (1) Å; **2b**, 2.597 (3) Å; **7a**, 2.502 (3) Å) and in the range of typical Fe–Fe single bonds.[17]

The 3-ferra-4-pyrrolin-2-one complex **2b** crystallizes in the space group $Pbc2_1$ (nonstandard $Pca2_1$) with two independent but structurally similar molecules per unit cell. The Fe atoms are bridged by the μ-HC=C(H)N(Ph)C(O) ligand, which is coordinated to Fe(1) via an allyl-type coordination of C(9), C(8), and N(1) and bound to Fe(2) via the "allyl" carbon C(9) and the carbonyl carbon C(7). The carbon atom C(9) is 0.17 (2) Å closer to Fe(2) than it is to Fe(1), consistent with it being σ-bound to Fe(2) and π-bound to Fe(1). As Figure 1 illustrates, the metallacycle is not planar. The carbonyl carbon C(7) lies 0.445 Å out of the least-squares plane defined by the other four atoms of the metallacycle, and the dihedral angle between the Fe(2)–C(9)–C(8)–N(1) plane and the Fe(2)–N(1)–C(7) plane is 25.4°. The C(8)–C(9) distance of 1.379 (20) Å is typical of a π-bonded olefin ligand[18] and corresponds to a bond order between 1 and 2.

(17) Krüger, C.; Barnett, B. L.; Brauer, D. In *The Organic Chemistry of Iron*; Koerner von Gustorf, E. A., Grevels, F.-W., Fischler, I., Eds.; Academic Press: New York, 1978; Vol. I, Chapter 1.

(18) Wells, A. F. *Structural Inorganic Chemistry*, 5th ed.; Oxford University Press: Oxford, 1984.

Table III. Crystal, Data Collection, and Refinement Parameters for $Fe_2(\mu\text{-CHCH=NHBu}^t)(CO)_6[CF_3SO_3]$ (**6a′**) and $[Fe_2(\mu\text{-C\{OMe\}=CHCH=NBu}^t)(CO)_6][BF_4]$ (**7a**)

	6a′	**7a**
	Crystal Parameters	
formula	$C_{15}H_{12}F_3Fe_2NO_{11}S$	$C_{14}H_{14}BF_4Fe_2NO_7$
fw	582.99	506.0
crystal system	monoclinic	orthorhombic
space group	$P2_1/n$	$P2_12_12_1$
a, Å	8.336 (1)	9.792 (4)
b, Å	15.879 (3)	14.623 (4)
c, Å	17.435 (3)	16.926 (4)
β, deg	99.30 (1)	
V, Å^3	2277.4 (7)	2423.8 (14)
Z	4	4
μ (Mo Kα), cm^{-1}	14.37	15.95
D_{calc}, g cm^{-3}	1.700	1.387
color	orange	golden yellow
size, mm	0.36 × 0.30 × 0.38	0.34 × 0.36 × 0.28
temp, K	296	296
	Data Collection	
diffractometer	Nicolet R3m	
monochromator	graphite	
scan method	Wyckoff	
radiation	Mo Kα	
wavelength, Å	0.71073	
scan lim, deg	$4 \le 2\theta \le 50$	$4 \le 2\theta \le 48$
data collected	±10, +19, +21	±12, +17, +20
reflectn collected	3977	4126
indepent reflectn	2688	4098
R_{int}, %	3.40	
obsvd reflectn	3969	1721
	$R_o \ge 5\sigma(F_o)$	$F_o \ge 5\sigma(F_o)$
	Refinement	
$R(f)$, %	4.78	6.78
$R(wf)$, %	4.80	6.10
$\Delta(\sigma)$, e Å^{-3}	0.62	0.799
Δ/σ_{max}	0.020	0.079
N_o/N_v	8.67	7.0
GOF	1.240	1.239

The 2,3-ferrazetine complex **3a** crystallized with two independent but structurally similar molecules in the asymmetric unit. Interestingly, one of these molecules possesses a puckered ferrazetine ring (maximum deviation: Fe(1), 0.077; N(1), 0.121; C(7), −0.127; C(8), 0.171 Å), while the other has a nearly planar ring (maximum deviation: Fe(1), −0.046; N(1), 0.065; C(7), 0.068; C(8), −0.088 Å). The bridging organic ligand of **3b** is π-coordinated to Fe(2) via C(7), C(8), and N(1) and bound to Fe(1) via the nitrogen atom and C(7). The C(7) carbon is 0.14 Å closer to Fe(1) than to Fe(2), consistent with it being σ-bound to the former metal and π-bound to the latter. The C(7)–C(8) distance of 1.369 (21) Å compares well to the corresponding distance in **2b**.

Complex **5b** is an isomer of **2b** and is structurally similar. The two Fe atoms are bridged by the μ_2,η^3-C(O)C(H)=C(H)NPh ligand, which is coordinated to Fe(2) via an allyl-type coordination of N, C(9), and C(8) and to Fe(1) via the carbonyl carbon C(7) and the nitrogen atom. Like **2b**, the metallacycle of **5b** is not planar with the carbonyl carbon C(7) lying 0.362 Å out of the least-squares plane defined by the other four atoms. The dihedral angle between the Fe(1)–N–C(9)–C(8) plane and the Fe(1)–C(7)–C(8) plane is 21.7°. The nitrogen atom symmetrically bridges the two metal atoms, while the ring carbonyl carbon is bonded only to Fe(1), with no apparent interaction with the other metal atom.

The complex **7a** crystallizes in the space group $P2_12_12_1$. The unit cell consists of **7a** and a disordered $CDCl_3$ molecule. The two Fe atoms are bridged by the μ_2,η^4-C(OCH$_3$)C(H)=C(H)-NBu^t ligand, which is coordinated via an allyl-type coordination of N, C(9), C(8), and C(7) to Fe(2) and via C(7) and N to Fe(1). Like **3a**, the metallacycle is a nearly planar ring (maximum deviation: Fe(1), −0.003; N, 0.023; C(7), −0.015; C(8), 0.033; C(9), −0.038 Å). Carbon atom C(7) is 0.325 (15) Å closer to

Table IV. Atomic Coordinates (×10⁴) and Isotropic Thermal Parameters (Å² × 10³) for $Fe_2(\mu\text{-CH=CHNPhC\{O\}})(CO)_6$ (**2b**)

	x	y	z	U[a]		x	y	z	U[a]
Fe(1)	4901 (1)	1575 (2)	5000	44.9 (7)	Fe(1′)	116 (1)	1056 (2)	2055 (2)	41.8 (7)
Fe(2)	3963 (1)	2166 (2)	6229 (3)	45.5 (8)	Fe(2′)	1044 (1)	517 (2)	3326 (2)	44.7 (8)
O(1)	[illegible]64 (6)	808 (11)	3863 (11)	91 (6)	O(1′)	−1048 (5)	1776 (8)	899 (10)	77 (5)
O(2)	[illegible]5)	3602 (8)	3951 (9)	68 (5)	O(2′)	160 (6)	−1021 (8)	1110 (10)	78 (5)
O(3)	[illegible]	4339 (11)	3635 (11)	95 (6)	O(3′)	1032 (6)	2061 (10)	600 (10)	98 (6)
O(4)	3550 [illegible]	4297 (8)	5741 (10)	80 (5)	O(4′)	1418 (6)	−1608 (10)	2808 (14)	103 (7)
O(5)	2853 (6)	1129 (11)	5169 (12)	112 (7)	O(5′)	2199 (6)	1539 (11)	2383 (12)	114 (7)
O(6)	3373 (5)	2037 (9)	8307 (10)	83 (5)	O(6′)	1500 (6)	577 (11)	5488 (11)	92 (6)
O(7)	4983 (5)	3592 (8)	6972 (9)	53 (4)	O(7′)	9 (5)	−851 (7)	4122 (7)	46 (3)
N(1)	5344 (5)	1997 (8)	6393 (11)	43 (4)	N(1′)	−326 (5)	758 (7)	3458 (9)	30 (4)
C(1)	5614 (8)	1119 (14)	4336 (13)	56 (7)	C(1′)	−592 (8)	1550 (13)	1382 (14)	68 (7)
C(2)	4821 (7)	2803 (12)	4373 (11)	50 (6)	C(2′)	171 (7)	−287 (13)	1462 (14)	66 (7)
C(3)	4365 (9)	877 (12)	4156 (2)	62 (7)	C(3′)	678 (8)	1640 (14)	1151 (15)	76 (7)
C(4)	3695 (7)	3457 (13)	5938 (12)	57 (6)	C(4′)	1277 (7)	−806 (12)	2971 (16)	62 (7)
C(5)	3288 (7)	1512 (13)	5542 (14)	62 (7)	C(5′)	1753 (8)	1140 (14)	2734 (14)	68 (7)
C(6)	3583 (7)	2112 (10)	7539 (17)	65 (7)	C(6′)	1346 (7)	571 (14)	4635 (18)	61 (7)
C(7)	4779 (7)	2802 (14)	6673 (12)	50 (6)	C(7′)	201 (7)	−57 (12)	3760 (11)	44 (6)
C(8)	5112 (7)	971 (12)	6449 (13)	54 (6)	C(8′)	−89 (7)	1773 (9)	3461 (12)	43 (5)
C(9)	4446 (7)	875 (11)	6260 (14)	56 (6)	C(9′)	576 (7)	1804 (11)	3305 (12)	52 (6)
C(10)	6297 (5)	2995 (9)	5925 (8)	67 (8)	C(10′)	−1301 (5)	−263 (8)	3056 (7)	45 (6)
C(11)	6935	3304	6127	86 (9)	C(11′)	−1951	−517	3242	70 (7)
C(12)	7271	2903	6985	82 (9)	C(12′)	−2303	−4	4019	90 (10)
C(13)	6969	2192	7643	82 (9)	C(13′)	−2003	763	4610	77 (8)
C(14)6	6331	1883	7441	60 (7)	C(14′)	−1353	1017	4424	54 (6)
C(15)	5995	2284	6583	57 (7)	C(15′)	−1002	504	3647	30 (5)

[a] Equivalent isotropic U defined as one-third of the trace of the orthogonalized U_{ij} tensor.

Table V. Selected Bond Distances and Angles for $Fe_2(\mu\text{-CH=CHNPhC\{O\}})(CO)_6$ (**2b**)

Bond Distances, Å			
Fe(1)–Fe(2)	2.597 (3)	Fe(1′)–Fe(2′)	2.596 (3)
Fe(1)–N(1)	2.096 (13)	Fe(1′)–N(1′)	2.042 (11)
Fe(1)–C(1)	1.792 (17)	Fe(1′)–C(1′)	1.808 (17)
Fe(1)–C(2)	1.798 (16)	Fe(1′)–C(2′)	1.913 (18)
Fe(1)–C(3)	1.788 (19)	Fe(1′)–C(3′)	1.798 (18)
Fe(1)–C(8)	2.053 (16)	Fe(1′)–C(8′)	2.063 (14)
Fe(1)–C(9)	2.069 (17)	Fe(1′)–C(9′)	2.092 (16)
Fe(2)–C(4)	1.811 (17)	Fe(2′)–C(4′)	1.849 (16)
Fe(2)–C(5)	1.848 (16)	Fe(2′)–C(5′)	1.829 (17)
Fe(2)–C(6)	1.844 (21)	Fe(2′)–C(6′)	1.799 (22)
Fe(2)–C(7)	1.953 (16)	Fe(2′)–C(7′)	1.966 (15)
Fe(2)–C(9)	1.955 (15)	Fe(2′)–C(9′)	1.935 (15)
O(7)–C(7)	1.176 (2)	O(7′)–C(7′)	1.201 (8)
N(1)–C(7)	1.605 (19)	N(1′)–C(7′)	1.566 (18)
N(1)–C(8)	1.423 (8)	N(1′)–C(8′)	1.411 (16)
C(8)–C(9)	1.394 (21)	C(8′)–C(9′)	1.379 (20)
Bond Angles, deg			
C(7)–Fe(2)–C(9)	85.7 (7)	C(7′)–Fe(2′)–C(9′)	84.1 (6)
C(7)–N(1)–C(8)	111.3 (11)	C(7′)–N(1′)–C(8′)	113.4 (10)
Fe(2)–C(7)–O(7)	140.6 (13)	Fe(2′)–C(7′)–O(7′)	136.5 (12)
Fe(2)–C(7)–N(1)	106.1 (10)	Fe(2′)–C(7′)–N(1′)	106.3 (9)
O(7)–C(7)–N(1)	112.8 (12)	O(7′)–C(7′)–N(1′)	117.1 (12)
N(1)–C(8)–C(9)	113.8 (13)	N(1′)–C(8′)–C(9′)	111.7 (11)
Fe(1)–C(9)–Fe(2)	80.3 (6)	Fe(1′)–C(9′)–Fe(2′)	80.2 (6)
Fe(2)–C(9)–C(8)	115.1 (11)	Fe(2′)–C(9′)–C(8′)	117.6 (10)

Fe(1) than to Fe(2), consistent with C(7) being σ-bonded to Fe(1) and π-bonded to Fe(2). The C(7)–C(8) distance of 1.381 (21) Å compares well with the corresponding distances in **2b** and **3b** and the C(8)–C(9) distance in **5b**.

Crystal and Molecular Structure of $[Fe_2\{\mu\text{-C(H)(CH=NHR)}\}(CO)_8][CF_3SO_3]$ (6a′). An ORTEP drawing of this salt is shown in Figure 4, and pertinent crystallographic details are given in Tables II, XII, and XIII. The salt consists of a $[Fe_2\{\mu\text{-C(H)(CH=NHR)}\}(CO)_8]^+$ cation linked by a hydrogen bond to the $CF_3SO_3^-$ anion (the O(10)···H(*n*) distance is 2.20 (4) Å for a $0.5 - x, -0.5 + y, 0.5 - z$ transformation of H(*n*)). The cation consists of two $Fe(CO)_4$ units joined by an Fe–Fe bond (2.646 (3) Å) bridged by the carbene carbon of the protonated azallylidene ligand. The Fe–Fe bond is slightly longer than the Fe–Fe bonds in the complexes described above but is still within the range of Fe–Fe single bonds.[17] The coordination geometry around each Fe atom is that of a distorted octahedron defined by the four CO

Scheme IV

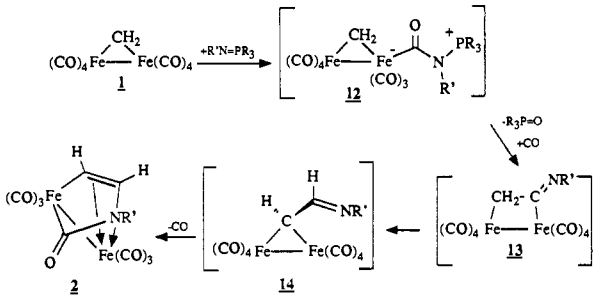

ligands, the adjacent Fe atom, and the C(9) atom of the bridging organic ligand. The short C(10)–N bond distance of 1.291 (5) Å is in the range of organic iminiums and indicates a localized double bond between these two atoms.[19] This structure contrasts with that of the isoelectronic complex $Fe_2(\mu\text{-CH}_2)(CO)_8$, which in the solid state possesses two bridging CO ligands and is isostructural with $Fe_2(CO)_9$.[20] However, the IR data of the latter compound indicate that, in solution, it rearranges to form an isomer without bridging CO's.[20]

Discussion

The most surprising finding in this research was the formation of the ferrapyrrolinone and ferrazetine complexes **2a,b** and **3a,b** upon treatment of $Fe_2(\mu\text{-CH}_2)(CO)_8$ with phosphine imides. The latter complexes were shown to arise from the former, and the mechanism proposed to explain the formation of the ferrapyrrolinone complexes is shown in Scheme IV. The initial step is believed to be phosphine imide addition to a metal carbonyl to give the acyl intermediate **12**. Ylides are known to add to metal carbonyls in this fashion to give similar acyl complexes,[21] and it has been suggested that this is the first step in the deoxygenation of metal carbonyls by phosphine imides.[1,2] Furthermore, evidence for this step comes from the reaction of $Fe_2(\mu\text{-CMe}_2)(CO)_8$ with $Bu^tN{=}P(Bu^n)_3$, which forms a compound formulated as $[Fe_2(\mu\text{-CMe}_2)(CO)_7\{C(O)N(Bu^t)P(Bu^n)_3\}]$ (**11**; eq 7) having an acyl ligand similar to that proposed for **12**.

(19) Sandorfy, C. In *Chemistry of the Carbon Nitrogen Double Bond*; Pattai, S., Ed.; Interscience Publishers: London, 1970; Chapter 1. Nyburg, S. C. *X-ray Analysis of Organic Structures*; Academic Press Inc.: New York, London, 1961.

(20) Sumner, C. E., Jr.; Riley, P. E.; Davis, R. E.; Pettit, R. *J. Am. Chem. Soc.* **1980**, *102*, 1752.

(21) Schmidbaur, H. *Angew. Chem., Int. Ed. Engl.* **1983**, *22*, 907.

Table VI. Atomic Coordinates (×10⁴) and Isotropic Thermal Parameters (Å² × 10³) for $Fe_2(\mu\text{-}CH{=}CHNBu^t)(CO)_6$ (**3a**)

	x	y	z	U[a]		x	y	z	U[a]
Fe(1)	2835 (2)	1617 (2)	1656.1 (6)	49.6 (8)	C(10)	6023 (18)	232 (19)	2076 (5)	109 (7)
Fe(2)	3628 (1)	3959 (2)	1860.0 (7)	59.0 (9)	C(11)	6856 (17)	2684 (18)	2227 (5)	96 (6)
Fe(1v)	5378 (2)	3092 (3)	4205.9 (7)	54 (1)	C(12)	6377 (15)	1820 (17)	1496 (5)	82 (5)
Fe(2′)	6260 (2)	724 (2)	4286.5 (7)	52.7 (9)	O(1′)	2558 (11)	2506 (17)	4057 (6)	178 (10)
N(1)	4542 (10)	2164 (12)	1944 (3)	47 (5)	O(2′)	5767 (10)	3720 (13)	3329 (3)	91 (5)
N(1′)	7181 (11)	2500 (11)	4429 (3)	45 (5)	O(3′)	5098 (16)	5919 (14)	4512 (4)	141 (8)
O(1)	24 (10)	2102 (14)	1466 (4)	97 (6)	O(4′)	3831 (11)	−880 (13)	4240 (4)	100 (6)
O(2)	3398 (11)	1254 (14)	779 (3)	98 (6)	O(5′)	6893 (12)	433 (12)	3407 (3)	104 (6)
O(3)	2587 (13)	−1311 (12)	1874 (4)	113 (6)	O(6′)	7946 (13)	−1575 (13)	4627 (5)	137 (7)
O(4)	1152 (11)	5541 (13)	1824 (4)	119 (6)	C(1′)	3648 (19)	2758 (20)	4092 (6)	101 (7)
O(5)	4300 (12)	4543 (13)	1007 (4)	112 (6)	C(2′)	5667 (13)	3498 (15)	3673 (4)	57 (4)
O(6)	5184 (12)	6131 (15)	2285 (5)	157 (8)	C(3′)	5208 (17)	4767 (19)	4395 (5)	93 (6)
C(1)	1150 (17)	1890 (17)	1526 (5)	69 (5)	C(4′)	4760 (17)	−282 (18)	4242 (5)	72 (5)
C(2)	3259 (15)	1372 (17)	1126 (5)	64 (5)	C(5′)	6684 (14)	533 (16)	3760 (5)	67 (5)
C(3)	2700 (16)	−127 (18)	1802 (5)	82 (5)	C(6′)	7285 (15)	−691 (17)	4506 (5)	71 (5)
C(4)	2137 (15)	4941 (18)	1847 (5)	79 (5)	C(7′)	5330 (16)	1888 (16)	4707 (5)	74 (5)
C(5)	4052 (14)	4313 (16)	1349 (4)	62 (4)	C(8′)	6619 (15)	2125 (16)	4796 (5)	74 (5)
C(6)	4609 (18)	5189 (20)	2120 (6)	99 (6)	C(9′)	8550 (15)	3074 (17)	4421 (5)	62 (5)
C(7)	2647 (15)	2480 (16)	2191 (5)	60 (5)	C(10′)	8550 (16)	4526 (17)	4564 (5)	89 (6)
C(8)	3959 (15)	2491 (15)	2311 (5)	68 (5)	C(11′)	9461 (16)	2184 (17)	4709 (5)	82 (5)
C(9)	5978 (15)	1733 (17)	1952 (5)	68 (5)	C(12′)	8958 (15)	2939 (17)	3980 (5)	80 (5)

[a] Equivalent isotropic U defined as one-third of the trace of the orthogonalized U_{ij} tensor.

Table VII. Selected Bond Distances and Angles for $Fe_2(\mu\text{-}CH{=}CHNBu^t)(CO)_6$ (**3a**)

Bond Distances, Å			
Fe(1)–Fe(2)	2.476 (3)	Fe(1′)–Fe(2′)	2.463 (3)
Fe(1)–N(1)	1.993 (10)	Fe(1′)–N(1′)	2.015 (11)
Fe(1)–C(7)	1.935 (16)	Fe(1′)–C(7′)	1.994 (16)
Fe(2)–N(1)	1.977 (11)	Fe(2′)–N(1′)	1.994 (11)
Fe(2)–C(7)	2.073 (16)	Fe(2′)–C(7′)	2.037 (16)
Fe(2)–C(8)	2.044 (16)	Fe(2′)–C(8′)	2.141 (16)
N(1)–C(8)	1.390 (20)	N(1′)–C(8′)	1.391 (20)
C(7)–C(8)	1.369 (21)	C(7′)–C(8′)	1.346 (23)
Bond Angles, deg			
N(1)–Fe(1)–C(7)	66.4 (6)	N(1′)–Fe(1′)–C(7′)	67.1 (6)
N(1)–Fe(2)–C(7)	64.1 (5)	N(1′)–Fe(2′)–C(7′)	66.6 (6)
N(1)–Fe(2)–C(8)	40.4 (6)	N(1′)–Fe(2′)–C(8′)	39.1 (5)
C(7)–Fe(2)–C(8)	38.8 (6)	C(7′)–Fe(2′)–C(8′)	37.5 (6)
Fe(1)–N(1)–Fe(2)	77.1 (4)	Fe(1′)–N(1′)–Fe(2′)	75.8 (4)
Fe(1)–N(1)–C(8)	93.0 (8)	Fe(1′)–N(1′)–C(8′)	88.0 (8)
Fe(2)–N(1)–C(8)	72.4 (8)	Fe(2′)–N(1′)–C(8′)	76.2 (8)
Fe(1)–N(1)–C(9)	138.3 (9)	Fe(1′)–N(1′)–C(9′)	135.7 (9)
Fe(2)–N(1)–C(9)	133.4 (9)	Fe(2′)–N(1′)–C(9′)	137.5 (9)
C(8)–N(1)–C(9)	120.5 (1)	C(8′)–N(1′)–C(9′)	122.7 (11)
Fe(1)–C(7)–Fe(2)	76.2 (6)	Fe(1′)–C(7′)–Fe(2′)	75.3 (6)
Fe(1)–C(7)–C(8)	96.3 (11)	Fe(1′)–C(7′)–C(8′)	90.1 (11)
Fe(2)–C(7)–C(8)	69.4 (9)	Fe(2′)–C(7′)–C(8′)	75.5 (10)
Fe(2)–C(8)–N(1)	67.2 (8)	Fe(2′)–C(8′)–N(1′)	64.7 (8)
Fe(2)–C(8)–C(7)	71.7 (9)	Fe(2′)–C(8′)–C(7′)	67.1 (9)
N(1)–C(8)–C(7)	102.5 (13)	N(1′)–C(8′)–C(7′)	108.0 (14)

The next step proposed in Scheme IV is coupling of the acyl and methylene ligands of **12** with concomitant elimination of phosphine oxide. This would give the μ-ketenimine complex **13**. The timing of the phosphine oxide elimination is uncertain. It may occur concurrent or subsequent to the acyl migration, but it is unlikely that it occurs prior to formation of the carbon–carbon bond of the ketenimine ligand. Direct phosphine oxide elimination from **12** would give the isocyanide-substituted complex $Fe_2(\mu\text{-}CH_2)(CO)_7(C{\equiv}NR)$, which could possibly undergo insertion of the isocyanide ligand into the Fe–methylene bond to give **13**. If so, the ferrapyrrolinone and ferrazetine complexes described herein should form by treating $Fe_2(\mu\text{-}CH_2)(CO)_8$ with isocyanides, but they do not. When $Bu^tN{\equiv}C$ was added to $Fe_2(\mu\text{-}CH_2)(CO)_8$, a mixture of products resulted in which the compounds $Fe(CO)_4(C{\equiv}NBu^t)$ and $Fe(CO)_3(C{\equiv}NBu^t)_2$ were identified (see Experimental Section) but no traces of **2a** or **3a** were detected. It should also be recalled that Keim has shown that $Fe_2(\mu\text{-}CH_2)(CO)_8$ reacts with NaOMe in the presence of CO to form methyl acetate, and it was proposed that this reaction involves as a key step the coupling of μ-CH_2 and –C{O}OMe ligands, the latter formed via nucleophilic attack of methoxide on a CO ligand to give an intermediate analogous to **12**.[7c]

To complete the sequence of reactions in Scheme IV, the μ-ketenimine ligand of **13** must then rearrange to the azallylidene ligand in **14**. The latter rearrangement is similar to rearrangements observed by Pettit in related compounds. For example, phenylacetylene was shown to react with complex **1** to give a μ_2,η^3-allyl complex resulting from insertion of the alkyne into an Fe–carbon bond of **1** followed by hydride migration (eq 8).[15] Also,

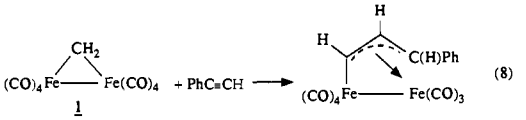

1 (8)

isopropylene was formed when complex **1** was treated with ethylene, and both of these transformations were proposed to proceed by a β-hydrogen elimination/readdition reaction se-

Table VIII. Atomic Coordinates (×10⁴) and Isotropic Thermal Parameters (Å² × 10³) for $Fe_2(\mu\text{-}C\{O\}CH{=}CHNPh)(CO)_6$ (**5b**)

	x	y	z	U[a]		x	y	z	U[a]
Fe(1)	4496.6 (4)	2272.9 (3)	2041.3 (3)	35.4 (1)	C(4)	5790 (4)	1756 (3)	4111 (2)	50 (1)
Fe(2)	5385.9 (4)	807.4 (3)	3196.9 (3)	36.4 (1)	C(5)	3502 (4)	519 (3)	3419 (2)	57 (1)
N	4963 (2)	789 (2)	1781 (2)	33 (1)	C(6)	6152 (4)	−347 (3)	3822 (2)	59 (1)
O(1)	4500 (3)	4230 (2)	3094 (2)	66 (1)	C(7)	6713 (3)	2371 (2)	2413 (2)	46 (1)
O(2)	4676 (4)	3431 (2)	331 (2)	82 (1)	C(8)	7308 (3)	1285 (2)	2555 (2)	44 (1)
O(3)	1126 (3)	2063 (2)	1854 (2)	74 (1)	C(9)	6433 (3)	502 (2)	2061 (2)	38 (1)
O(4)	6079 (3)	2345 (2)	4693 (2)	77 (1)	C(11)	3026 (2)	415 (1)	459 (1)	43 (1)
O(5)	2326 (3)	328 (3)	3570 (2)	91 (1)	C(12)	2153	−288	−129	54 (1)
O(6)	6596 (5)	−1043 (2)	4272 (2)	103 (2)	C(13)	2281	−1371	33	59 (1)
O(7)	7529 (3)	3136 (2)	2604 (2)	69 (1)	C(14)	3282	−1751	784	54 (1)
C(1)	4447 (4)	3447 (2)	2700 (2)	47 (1)	C(15)	4154	−1047	1373	44 (1)
C(2)	4586 (4)	2962 (2)	979 (2)	50 (1)	C(16)	4027	36	1210	34 (1)
C(3)	2409 (4)	2095 (2)	1907 (2)	45 (1)					

[a] Equivalant isotropic U defined as one-third of the trace of the orthogonalized U_{ij} tensor.

Table IX. Selected Bond Distances and Angles for $Fe_2(\mu\text{-}C\{O\}CH{=}CHNPh)(CO)_6$ (**5b**)

Bond Distances, Å			
Fe(1)–Fe(2)	2.557 (1)	Fe(1)–N	1.974 (2)
Fe(1)–C(7)	1.978 (3)	Fe(2)–N	2.046 (2)
Fe(2)–C(8)	2.157 (3)	Fe(2)–C(9)	2.054 (3)
N–C(9)	1.365 (3)	O(7)–C(7)	1.221 (4)
C(7)–C(8)	1.478 (4)	C(8)–C(9)	1.397 (4)
Bond Angles, deg			
N–Fe(1)–C(7)	83.2 (1)	Fe(1)–Fe(2)–C(8)	72.5 (1)
N–Fe(2)–C(8)	66.8 (1)	N–Fe(2)–C(9)	38.9 (1)
C(8)–Fe(2)–C(9)	38.6 (1)	Fe(1)–N–Fe(2)	79.0 (1)
Fe(1)–N–C(9)	114.6 (2)	Fe(2)–N–C(9)	70.9 (2)
Fe(1)–N–C(16)	128.2 (1)	Fe(2)–N–C(16)	126.5 (1)
C(9)–N–C(16)	116.4 (2)	Fe(1)–C(7)–O(7)	130.7 (2)
Fe(1)–C(7)–C(8)	107.7 (2)	O(7)–C(7)–C(8)	121.2 (3)
Fe(2)–C(8)–C(7)	91.7 (2)	Fe(2)–C(8)–C(9)	66.7 (2)
C(7)–C(8)–C(9)	115.2 (2)	Fe(2)–C(9)–N	70.2 (2)
Fe(2)–C(9)–C(8)	74.7 (2)	N–C(9)–C(8)	114.0 (2)

quence.[15] We suggest that a similar rearrangement occurs to form the azallylidene complex **14**. Once formed, nucleophilic attack of the phosphine imide nitrogen on a CO ligand of **14** would yield the observed ferrapyrrolinone product **2** after CO loss. Support for this next step comes from the finding that the protonated azallylidene complex **6** gives quantitative formation of **2** upon deprotonation with Et_3N (eq 6).

Another surprising finding in this research is the condition-dependent carbonylation behavior of the ferrazetine complexes **3a,b**. Recall that, under photochemical conditions, carbonylation occurred to form the 3-ferra-4-pyrrolin-2-one complexes **2a,b**, whereas under thermal conditions carbonylation occurred to form the isomeric 2-ferra-4-pyrrolin-3-one complexes **5a,b** (eq 9). These

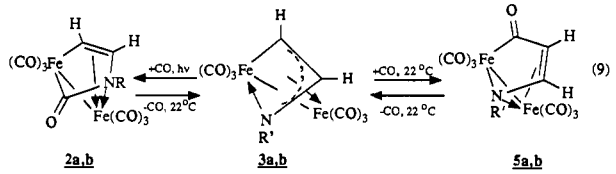

reactions may be rationalized by assuming that photolysis causes dissociation of the nitrogen atom from the metal to which it is datively bound followed by its attack on a CO ligand to give complexes **2a,b**. A recent low-temperature photolysis study of **3** supports this assumption.[22] The thermal reaction can best be rationalized as a normal CO insertion into a metal carbonyl bond to form an acyl ligand. However, this latter reaction is strongly affected by the substituent on the nitrogen atom since **3b** (R = Ph) can be quickly and quantitatively transformed into **5b**, whereas **3a** (R = Bu^t) slowly reacts with CO to form an equilibrium mixture of **3a** and **5a**, which favors the former.

In conclusion, the above described reaction of $Fe_2(\mu\text{-}CH_2)(CO)_8$ with phosphine imides has given entry into an impressive array of new binuclear complexes that possess a variety of organic ligands bridging the metal atoms. These ligands can be interconverted by carbonylation/decarbonylation and protonation/deprotonation reactions, and as described in preliminary communications[23,24] they can be further elaborated through their reactions with alkynes. Further studies aimed at inducing additional transformations of these complexes through their reactions with other organic and inorganic substrates are in progress.

Experimental Section

General. The compounds $Fe_2(\mu\text{-}CH_2)(CO)_8$ (**1**),[15] $Fe_2(\mu\text{-}CMe_2)(CO)_8$,[15] $Ph_3P{=}NPh$,[25] $(Bu^n)_3P{=}NBu^t$[25] were prepared by literature methods, and the reagents K[HB(*s*-Bu)$_3$], Bu^{t}N≡C, HBF_4, Et_3N, and [PPN]Cl were purchased from Aldrich Chemical Co. The salts [PPN]I and [PPN]Br were prepared from [PPN]Cl and the appropriate alkali-metal halide by precipitation from H_2O and recrystallized from acetone/Et_2O. Solvents were dried by stirring over Na/benzophenone (pentane, tetrahydrofuran, toluene) or CaH_2 (CH_2Cl_2) and freshly distilled prior to use. Complex **1** (350 mg, 1 mmol) was enriched in ^{13}CO by stirring in CH_2Cl_2 (30 mL) in a 50-mL Schlenk flask under 1 atm of ^{13}CO (99%) for 4 days. All manipulations were performed with standard Schlenk techniques unless otherwise specified. IR spectra were recorded on an IBM FTIR-32 spectrometer operated in the absorption mode, NMR spectra were obtained on a Bruker AM 300 FT NMR spectrometer, and electron impact (EI) and fast atom bombardment (FAB) mass spectra were recorded on AEI-MS9 and AFAB-MS9 mass spectrometers, respectively. Elemental analyses were obtained from Schwarzkopf Microanalytical Laboratories, Woodside, NY.

Reaction of $Fe_2(\mu\text{-}CH_2)(CO)_8$ (1) with $(Bu^n)_3P{=}NBu^t$. Complex **1** (200 mg, 0.57 mmol) was dissolved in CH_2Cl_2 (60 mL), and the solution was thoroughly saturated with CO by bubbling for 10 min. The reagent $(Bu^n)_3P{=}NBu^t$ (104 μL, 87.4 mg, 0.32 mmol) was then added dropwise to the solution, which gave a rapid color change to dark red. After the solution was stirred for an additional 2 h, the solvent was evaporated and the residue chromatographed on a Florisil column cooled to −30 °C with pentane as eluent. This gave an orange band of **3a** (39 mg, 0.10 mmol, 18%) followed by a second orange band of **2a** (160 mg, 0.40 mmol, 69%) when the eluent was changed to 2:1 pentane/CH_2Cl_2. A further change in eluent to 1:1 pentane/CH_2Cl_2 brought down a brown band of complex **4a** (11 mg, 0.023 mmol, 4%). Complexes **2a** and **3a** were isolated as microcrystalline solids, while **4a** was isolated as a brown oil by evaporating the solvent from the chromatography fractions.

Data for 2a. Anal. Calcd for $C_{13}H_{11}Fe_2NO_7$: C, 38.56; H, 2.74. Found: C, 38.37; H, 2.60. IR (CH_2Cl_2): ν_{CO} 2079 (m), 2036 (vs), 2008 (s), 1985 (sh), 1690 (w) cm^{-1}. EIMS: *m/z* 405 (M^+), fragment ions corresponding to loss of six CO ligands. ^1H NMR (acetone-d_6): δ 7.92 (d, 1 H, *J* = 4.5 Hz, C*H*=CHNBu^t), 7.48 (d, 1 H, CH=C*H*NBu^t), 1.43 (s, 9 H, Bu^t). ^{13}C NMR (CD_2Cl_2): δ 209.9, 209.1 (*C*O), 145.7 (dd, $^1J_{CH}$ = 161.7 Hz, $^2J_{CH}$ = 3.0 Hz, *C*H=CHNBu^t), 102.9 (dd, $^1J_{CH}$ = 189.4 Hz, $^2J_{CH}$ = 5.3 Hz, -CH=*C*HNBu^t), 58.1 (*C*Me$_3$), 30.4 (C(*C*H$_3$)$_3$).

Data for 3a. Anal. Calcd for $C_{12}H_{11}Fe_2NO_6$: 38.24; H, 2.94. Found: C, 37.95; H, 3.06. IR (CH_2Cl_2): ν_{CO} 2069 (m), 2024 (vs), 1983 (s) cm^{-1}. EIMS *m/z* 377 (M^+), fragment ions corresponding to loss of six carbonyl ligands. ^1H NMR (CD_2Cl_2): δ 6.52 (d, *J* = 2.1 Hz, 1 H, -CH=C*H*NBu^t), 5.98 (d, 1 H, -C*H*=CHNBu^t), 1.02 (s, Bu^t). ^{13}C NMR (CD_2Cl_2): δ 211.5 (*C*O), 111.5 (dd, $^1J_{CH}$ = 176.7 Hz, $^2J_{CH}$ = 5.3 Hz, -CH=*C*HNBu^t), 110.3 (dd, $^1J_{CH}$ = 174.1 Hz, $^2J_{CH}$ = 2.5 Hz, -*C*H=CHNBu^t), 58.1 (*C*Me$_3$), 30.4 (C(*C*H$_3$)$_3$).

Data for 4a. IR (CH_2Cl_2): ν_{CO} = 2164 (m), 2044 (s), 1997 (vs), 1969 (s), 1961 (s) cm^{-1}. EIMS: *m/z* 460 (M^+), fragment ions corresponding to loss of six carbonyl ligands. ^1H NMR (CD_2Cl_2): δ 7.10 (d, *J* = 4.6 Hz, 1 H, C*H*), 6.78 (d, 1 H, C*H*), 1.52 (s, Bu^t), 1.39 (s, Bu^t). ^{13}C NMR (CD_2Cl_2): δ 214.0, 213.0, 210.4 (*C*≡NBu^t and *C*O ligands), 141.2 (*C*H), 101.2 (*C*H), 58.9 (*C*Me$_3$), 58.1 (*C*Me$_3$), 30.6 (C(*C*H$_3$)$_3$), 29.2 (C(*C*H$_3$)$_3$).

Reaction of $Fe_2(\mu\text{-}CH_2)(CO)_8$ (1) with $Ph_3P{=}NPh$. Complex **1** (250 mg, 0.71 mmol) was dissolved in 150 mL of CH_2Cl_2, and the solution was saturated with bubbling CO for 10 min followed by dropwise addition of $Ph_3P{=}NPh$ (265 mg, 0.75 mmol) dissolved in 10 mL of CH_2Cl_2. The solution turned red, and after it was stirred for 2 h the solvent was evaporated. Chromatography of the residue on a silica gel column cooled to −30 °C with pentane as eluent gave elution of a small orange band of **3b** (12 mg, 0.03 mmol, 4%). The solvent was then changed to 2:1 pentane/CH_2Cl_2 to elute an orange band of **2b** (218 mg, 0.51 mmol, 72%). When the eluent was changed to 1:1 pentane/CH_2Cl_2, a light brown band of **4b** (1 mg, <1%) eluted.

Data for 2b. Anal. Calcd for $C_{15}H_7Fe_2NO_7$: C, 42.40; H, 1.66. Found: C, 41.98; H, 1.99. IR (CH_2Cl_2): ν_{CO} 2079 (m), 2037 (vs), 2007 (s), 1983 (sh) 1690 cm^{-1}. EIMS: *m/z* 425 (M^+), fragment ions corresponding to loss of six carbonyl ligands. ^1H NMR (C_6D_6): δ 6.79–6.51 (m, Ph), 7.47 (d, 1 H, *J* = 4.1 Hz, C*H*=CHNPh), 5.98 (d, 1 H, CH=C*H*NPh). ^{13}C NMR (C_6D_6): δ 210.7, 209.8 (CO), 148.4 (dd, *C*H=CHNPh, $^1J_{CH}$ = 161.1 Hz, $^2J_{CH}$ = 3.6 Hz), 139.7, 129.1, 126.2 (Ph), 101.1 (dd, CH=*C*HNPh, $^1J_{CH}$ = 189.3 Hz, $^2J_{CH}$ = 5.0 Hz). The δ 101.1 resonance was assigned to the CH=*C*HNPh carbon on the basis of its intensity enhancement when **2a** was prepared from ^{13}CO-enriched **1** (see Discussion).

Data for 3b. Anal. Calcd for $C_{14}H_7Fe_2NO_6$: C, 42.37; H, 1.78. Found: C, 42.13; H, 1.82. IR (CH_2Cl_2): ν_{CO} 2069 (m), 2030 (vs), 1990 (s) cm^{-1}. EIMS: *m/z* 397 (M^+), fragment ions corresponding to loss

(22) Mirkin, C. A.; Oyer, T. J.; Wrighton, M. S.; Snead, T. E.; Geoffroy, G. L. To be submitted for publication.
(23) Mirkin, C. A.; Kuang-Lieh, Lu; Snead, T. E.; Geoffroy, G. L.; Rheingold, A. L. *J. Am. Chem. Soc.* **1990**, *112*, 2809.
(24) Mirkin, C. A.; Kuang-Lieh, Lu; Geoffroy, G. L.; Rheingold, A. L. *J. Am. Chem. Soc.* **1990**, *112*, 461. As corrected in Mirkin, C. A.; Kuang-Lieh, Lu; Geoffroy, G. L.; Rheingold, A. L. *J. Am. Chem. Soc.* **1990**, *112*, 6155.
(25) Wiegräbe, W.; Bock, H. *Chem. Ber.* **1968**, *101*, 1414.

Table X. Atomic Coordinates (×10⁴) and Isotropic Thermal Parameters (Å² × 10³) for [Fe₂(μ-C{OMe}CHCHNBu^t)(CO)₆][BF₄] (7a)

	x	y	z	U[a]		x	y	z	U[a]
Fe(1)	8310.5 (18)	7475.5 (15)	4654.4 (12)	41.9 (7)*	O(3)	10944 (10)	1636 (7)	5077 (6)	67 (5)*
Fe(2)	7223.0 (19)	1390.5 (15)	3437.3 (13)	45.0 (8)*	O(4)	8721 (10)	2965 (7)	4063 (7)	73 (5)*
C(1)	7623 (12)	1330 (9)	5520 (7)	39 (4)	O(5)	7592 (16)	2015 (12)	1812 (8)	140 (8)*
C(2)	8608 (18)	−270 (14)	5146 (11)	74 (6)	O(6)	4548 (10)	2218 (8)	3590 (8)	100 (6)*
C(3)	9973 (13)	1267 (10)	4863 (8)	47 (4)	O(7)	4572 (8)	515 (8)	4891 (6)	71 (5)*
C(4)	8138 (13)	2338 (9)	3860 (8)	48 (4)	N	8659 (9)	370 (7)	3548 (6)	41 (4)*
C(5)	7413 (17)	1769 (12)	2440 (10)	78 (6)	B	5925 (10)	4681 (7)	3130 (6)	57 (6)
C(6)	5624 (16)	1917 (12)	3512 (10)	77 (6)	F(1)	6504 (10)	3913 (7)	2858 (7)	141 (6)*
C(7)	6481 (15)	377 (1)	4353 (9)	61 (5)	F(2)	6117 (9)	5335 (7)	2606 (6)	126 (6)*
C(8)	6349 (14)	86 (10)	3581 (9)	50 (4)	F(3)	6527 (9)	4917 (7)	3815 (5)	105 (5)*
C(9)	7527 (13)	27 (10)	3174 (8)	40 (4)	F(4)	4586 (8)	4532 (7)	3240 (5)	98 (5)*
C(10)	4119 (15)	169 (11)	4681 (11)	87 (6)	C(21)	3117 (19)	2109 (13)	1089 (11)	98 (7)*
C(11)	10049 (14)	277 (11)	3093 (9)	53 (5)	Cl(1A)	3351 (17)	2733 (8)	1920 (8)	154 (7)*
C(12)	9856 (17)	−119 (11)	2300 (9)	81 (6)	Cl(1B)	4431 (15)	2771 (8)	1437 (10)	166 (8)*
C(13)	10077 (15)	1161 (10)	3074 (9)	66 (5)	Cl(2A)	3811 (12)	2616 (10)	279 (9)	160 (7)*
C(14)	10819 (16)	−395 (12)	3611 (10)	90 (6)	Cl(2B)	3123 (13)	2095 (8)	28 (7)	132 (6)*
O(1)	7123 (10)	1646 (8)	6035 (6)	73 (5)*	Cl(3A)	1276 (5)	2019 (10)	936 (8)	159 (7)*
O(2)	8756 (12)	−987 (8)	5459 (8)	95 (6)*	Cl(3B)	1586 (14)	2498 (10)	1339 (8)	173 (8)

[a] Equivalent isotropic U defined as one-third of the trace of the orthogonalized U_{ij} tensor indicated by asterisk.

Table XI. Selected Bond Distances and Angles for [Fe₂(μ-C{OMe}CHCHNBu^t)(CO)₆][BF₄] (7a)

Bond Distances, Å			
Fe(1)–Fe(2)	2.502 (3)	Fe(1)–N	1.981 (11)
Fe(1)–C(7)	1.939 (14)	Fe(2)–N	2.059 (10)
Fe(2)–C(8)	2.104 (14)	Fe(2)–C(7)	2.264 (16)
Fe(2)–C(9)	2.064 (15)	O(7)–C(7)	1.359 (18)
C(7)–C(8)	1.381 (21)	C(8)–C(9)	1.346 (19)
N–C(9)	1.327 (16)	N–C(11)	1.569 (17)
O(7)–C(10)	1.462 (17)		
Bond Angles, deg			
N–Fe(1)–C(7)	80.4 (5)	N–Fe(2)–C(7)	71.5 (5)
N–Fe(2)–C(8)	67.1 (5)	N–Fe(2)–C(9)	38.9 (5)
Fe(1)–C(7)–O(7)	117.0 (10)	C(7)–O(7)–C(10)	116.4 (12)
Fe(2)–C(7)–O(7)	126.5 (11)	C(8)–C(7)–O(7)	127.7 (13)
Fe(1)–Fe(2)–C(7)	47.7 (4)	Fe(1)–Fe(2)–C(8)	74.8 (4)
Fe(1)–Fe(2)–C(9)	75.7 (4)	Fe(1)–Fe(2)	50.4 (3)
C(7)–Fe(2)–C(8)	36.6 (6)	C(7)–Fe(2)–C(9)	64.0 (5)
C(8)–Fe(2)–C(9)	37.7 (5)	Fe(1)–C(7)–C(8)	114.9 (11)
C(7)–C(8)–C(9)	115.1 (3)	C(8)–C(9)–N	115.6 (12)
Fe(1)–N–C(9)	113.5 (8)	Fe(2)–N–C(9)	70.8 (7)
Fe(1)–N–C(11)	129.6 (8)	Fe(2)–N–C(11)	127.6 (8)
C(9)–N–C(11)	116.2 (11)		

of six CO ligands. ^{1}H NMR (C_6D_6): δ 6.68–6.56 (m, Ph), 5.84 (d, 1 H, J = 2.1 Hz, CH=C*H*NPh), 5.53 (d, 1 H, C*H*=CHNPh). ^{13}C NMR (C_6D_6): δ 210.7 (*C*O), 150.1, 131.6, 129.5, 126.5 (Ph), 113.3 (dd, $^1J_{CH}$ = 173.6 Hz, $^2J_{CH}$ = 3.0 Hz, CH=*C*HNPh), 109.3 (dd, $^1J_{CH}$ = 180.8 Hz, $^2J_{CH}$ = 5.9 Hz, *C*H=CHNPh).

Data for 4b. IR (CH_2Cl_2): ν_{CO} 2162 (m), 2044 (s), 1998 (vs), 1969 (s), 1961 (s) cm^{-1}.

Decarbonylation of 2a and 2b To Form 3a and 3b. Complex **2a** (100 mg, 0.29 mmol) was dissolved in THF (50 mL) in 250-mL flask. After the solution was stirred vigorously for 6 at 22 °C under N_2, IR analysis indicated the complete transformation of **2a** into **3a**, which was isolated by chromatography on Florisil at −30 °C with pentane eluent. Under similar conditions, complex **2b** (203 mg, 0.48 mmol) was transformed into **3b** in 4 days (160 mg, 0.40 mmol, 84%). Alternatively, complex **2a** (100 mg, 0.29 mmol) was dissolved in 30 mL of THF and heated to 50 °C under a N_2 purge. IR monitoring indicated quantitative conversion to **3a** after 3 h. Under similar conditions, complex **2b** (100 mg, 0.24 mmol) gave quantitative conversion to **4b**.

Halide- and Hydride-Promoted Transformation of 2 into 3. A 30-mL THF solution (0.002 M) of **2a** or **2b** was placed in a 50-mL Schlenk flask. To each reaction vessel was added a catalytic amount (10%) of [PPN]X (X = Cl$^-$, Br$^-$, I$^-$), predissolved in 1 mL of CH_2Cl_2, or 3 mL of a THF solution (0.002 M) of K[B(*s*-Bu)$_3$H]. Stirring was commenced, and the reaction was monitored by IR. As the 2079 cm^{-1} band of complex **2a** and **2b** decreased in intensity, the 2069 cm^{-1} band of **3a** and **3b** grew in. A plot of the log of absorbance at 2079 cm^{-1} of **2a** or **2b** versus time gave a straight line from which the pseudo-first-order rate constant, and $t_{1/2}$'s were obtained by a linear least-squares analysis.

Photoinduced Carbonylation of 3a,b To Form 2a,b. A 30-mL CH_2Cl_2 solution of **3a** (30 mg, 0.080 mmol) was placed in a 50-mL Schlenk flask. The flask was charged with 1 atm of CO and irradiated with an unfiltered Hanovia 450-W medium-pressure Hg discharge lamp for 30 min. IR analysis showed complete conversion to **2a**, which was isolated in 95% yield after filtering and evaporation of solvent. A similar procedure gave complex **2b** in 87% yield.

Carbonylation of 3a,b To Form 5a,b. A CH_2Cl_2 solution of complex **4b** (100 mg, 0.25 mmol) was placed in a 250-mL Schlenk flask and stirred under 1 atm of CO at room temperature for 1 h. The solvent was then allowed to slowly evaporate to yield red crystals of **5b** (76 mg, 0.18 mmol, 72%). Complex **5a** was formed by dissolving **3a** (20 mg, 0.049 mmol) in CD_2Cl_2 in a resealable NMR tube that was subsequently charged with 1 atm of CO. NMR monitoring showed the gradual buildup in concentration of **5a** at the expense of **3a** until equilibrium was reached after 2 days. The persistent presence of **3a** prevented isolation

Table XII. Atomic Coordinates (×10⁴) and Isotropic Thermal Parameters (Å² × 10³) for [Fe₂(μ-CHCH=NHBu^t)(CO)₈][CF₃SO₃] (6a′)

	x	y	z	U[a]		x	y	z	U[a]
Fe(1)	−1607.4 (8)	9149.5 (4)	1507.3 (3)	43.2 (2)	C(1)	−1303 (6)	8456 (3)	2365 (3)	53 (2)
Fe(2)	−3017.0 (8)	10349.0 (4)	2215.6 (4)	43.5 (2)	C(2)	−1828 (7)	9796 (3)	637 (3)	63 (2)
S	3395 (2)	7613.7 (9)	2935.4 (7)	63.0 (5)	C(3)	−3407 (7)	8562 (3)	1074 (3)	67 (2)
N	1356 (4)	10613 (2)	3217 (2)	40 (1)	C(4)	103 (7)	8624 (3)	1183 (3)	58 (2)
H(*n*)	1518 (47)	10990 (25)	2968 (22)	42 (11)	C(5)	−3022 (7)	11125 (4)	1429 (3)	61 (2)
C	3562 (8)	7380 (4)	3965 (3)	74 (2)	C(6)	−3098 (6)	9617 (3)	3008 (3)	51 (2)
O(1)	−1062 (5)	8000 (2)	2863 (2)	67 (1)	C(7)	−2873 (6)	11201 (3)	2917 (3)	50 (2)
O(2)	−1916 (7)	10160 (3)	73 (2)	101 (2)	C(8)	−5210 (6)	10173 (4)	1900 (3)	62 (2)
O(3)	−4561 (6)	8228 (3)	804 (3)	109 (2)	C(9)	−604 (5)	10134 (3)	2127 (2)	40 (1)
O(4)	1162 (5)	8303 (3)	976 (2)	87 (2)	C(10)	298 (5)	10074 (3)	2893 (3)	38 (1)
O(5)	−3105 (6)	11623 (3)	961 (2)	87 (2)	C(11)	2175 (5)	10639 (3)	4039 (2)	39 (1)
O(6)	−3179 (5)	9216 (2)	3544 (2)	72 (2)	C(12)	1461 (6)	11390 (3)	4417 (3)	63 (2)
O(7)	−2737 (5)	11691 (2)	3386 (2)	70 (1)	C(13)	1902 (7)	9826 (3)	4452 (3)	62 (2)
O(8)	−6538 (4)	10052 (3)	1692 (2)	93 (2)	C(14)	3981 (5)	10772 (4)	4020 (3)	76 (2)
O(10)	2257 (5)	7009 (3)	2571 (2)	85 (2)	F(10)	4021 (5)	6590 (2)	4129 (2)	105 (2)
O(11)	2847 (5)	8468 (2)	2889 (2)	85 (2)	F(11)	4567 (6)	7880 (3)	4394 (2)	126 (2)
O(12)	5016 (5)	7454 (3)	2774 (3)	101 (2)	F(12)	2136 (6)	7483 (3)	4203 (2)	129 (2)

[a] Equivalent isotropic U defined as one-third of the trace of the orthogonalized U_{ij} tensor.

Table XIII. Selected Bond Distances and Angles for $[Fe_2(\mu\text{-}CHCH{=}NHBu^t)(CO)_8][CF_3SO_3]$ (**6a'**)

Bond Distances, Å			
Fe(1)–Fe(2)	2.646 (1)	Fe(1)–C(9)	2.005 (4)
Fe(2)–C(9)	2.070 (4)	C(9)–C(10)	1.426 (6)
N–H(*n*)	0.77 (4)	N–C(10)	1.291 (5)
N–C(11)	1.486 (5)		
Bond Angles, deg			
Fe(2)–Fe(1)–C(9)	50.6 (1)	Fe(1)–Fe(2)–C(9)	48.4 (1)
C(10)–N–C(11)	128.0 (4)	Fe(1)–C(9)–Fe(2)	81.0 (2)
Fe(1)–C(9)–O(10)	124.3 (3)	Fe(2)–C(9)–C(10)	108.2 (3)
N–C(10)–C(9)	125.7 (4)		

of a pure sample of **5a**. A similar NMR experiment with **4b** showed quantitative formation of **5b** after 1 h.

Data for 5a. ^1H NMR (CD_2Cl_2): δ 7.24 (d, 1 H, C*H*, J = 2.8 Hz), 4.21 (d, 1 H, C*H*, J = 2.8 Hz), 1.49 (s, 9 H, C(CH_3)$_3$). ^{13}C NMR (CD_2Cl_2): δ 212.3, 211.3, 209.8 (*C*O), 184.6 (Fe*C*{O}N–), 119.1 (dd, $^1J_{CH}$ = 181.6 Hz, $^2J_{CH}$ = 7.63 Hz, *C*H), 74.8 (dd, $^1J_{CH}$ = 169.4 Hz, $^2J_{CH}$ = 9.2 Hz, *C*H), 65.2 (*C*Me$_3$), 33.9 (m, C(*C*H$_3$)$_3$, J_{CH} = 123.0 Hz).

Data for 5b. Anal. Calcd for $C_{15}H_7Fe_2NO_7$: 42.40; H, 1.66. Found: C, 42.10; H, 1.59. IR (CH_2Cl_2): ν_{CO} 2079 (m), 2037 (vs), 2007 (s), 1983 (sh) cm^{-1}. ^1H NMR (CD_2Cl_2): δ 7.40–7.18 (m, Ph), 7.28 (d, 1 H, C*H*, J = 2.5 Hz), 4.38 (d, 1 H, C*H*, J = 2.5 Hz). ^{13}C NMR (CD_2Cl_2): δ 211.6, 210.1, 206.9 (*C*O), 152.9, 130.0, 128.8, 125.7 (Ph), 121.6 (dd, *C*H, $^1J_{CH}$ = 187.7 Hz, $^2J_{CH}$ = 9.2 Hz), 77.3 (dd, *C*H, $^1J_{CH}$ = 169.4, $^2J_{CH}$ = 10.7).

Decarbonylation of Complex 5b To form 3b. A CH_2Cl_2 solution of complex **5b** (25 mg, 0.06 mmol) was placed in a 50-mL Schlenk flask. The flask was purged with N_2 until IR and ^1H NMR analysis indicated complete formation of **3b**.

Preparation of 6a,b by Protonation of 2a,b with HBF_4. Complex **2a** (463 mg, 1.14 mmol) in 50 mL of CH_2Cl_2 was generated in situ as described above. An Et_2O solution of HBF_4 (0.292 mL, 2.74 mmol) was added dropwise to the solution to induce a gradual color change from orange to dark red. After 30 min, the solution was concentrated by solvent evaporation and the product precipitated by adding Et_2O. The solid residue was separated from the supernatant, redissolved in CH_2Cl_2, and again precipitated by adding Et_2O. This procedure was repeated several times to ultimately yield pure **6a** (450 mg, 0.87 mmol, 76%) as an orange microcrystalline solid. A similar experiment with **2b** (172 mg, 0.41 mmol) led to the formation of **6b** in 81% yield (178 mg, 0.33 mmol).

Data for 6a. Anal. Calcd for $C_{14}H_{12}BF_4Fe_2NO_8$: C, 32.29; H, 2.13. Found: C, 32.02; H, 2.52. IR (CH_2Cl_2): ν_{CO} 2121 (w), 2078 (s), 2059 (m), 2039 (s) cm^{-1}; $\nu_{C=N}$ 1620 cm^{-1}. ^1H NMR (CD_2Cl_2): δ 10.26 (br, 1 H, C=N*H*Bu^t), 7.63 (dd, 1 H, J = 15.9, 13.4 Hz, C*H*=NHBu^t), 5.99 (d, 1 H, J = 13.4 Hz, μ-C*H*), 1.46 (s, 9 H, Bu^t). ^{13}C NMR (CD_2Cl_2): δ 205.8 (*C*O), 177.9 (dd, J_{CH} = 166.4 Hz, $^2J_{CH}$ = 6.1 Hz, μ-*C*HCH=NHBu^t), 89.4 (m, $^1J_{CH}$ = 146.5 Hz, μ-*C*HCH=NHBu^t), 58.7 (*C*Me$_3$), 28.5 (C(*C*H$_3$)$_3$). The δ 177.9 and 89.4 assignments were confirmed by a CH correlation experiment, which showed that these resonances respectively correlated with the δ 7.63 and 5.99 ^1H NMR signals.

Data for 6b. Anal. Calcd for $C_{16}H_8BF_4Fe_2NO_8$: C, 35.54; H, 1.49. Found: C, 35.54; H, 1.63. IR (CH_2Cl_2): ν_{CO} 2122 (m), 2079 (s), 2062 (sh), 2035 (vs) cm^{-1}. ^1H NMR (CD_2Cl_2): 11.68 (br, 1 H, N*H*Ph), 8.04 (m, 1 H, C*H*=NHPh), 7.51–7.36 (Ph), 6.22 (d, 1 H, J = 13.6 Hz, μ-C*H*). ^{13}C NMR (CD_2Cl_2): δ 205.3 (*C*O), 175.5 (dd, $^1J_{CH}$ = 173.9 Hz, $^2J_{CH}$ = 3.1 Hz, μ-CH*C*H=NHPh), 136.0, 131.0, 129.9, 120.1 (Ph), 89.9 (m, $^1J_{CH}$ = 146.5 Hz, μ-*C*HCH=NHPh).

Deprotonation of 6a,b with NEt_3 To Form 2a,b. Complex **6a** (100 mg, 0.19 mmol) was dissolved in 50 mL of THF, which was then saturated with CO by bubbling for 10 min. To this solution was added dropwise 1 equiv of NEt_3 to give an immediate color change from red to orange. IR spectroscopy showed quantitative transformation to **6a**. Chromatography on silica gel at −30 °C with 2:1 pentane/CH_2Cl_2 as eluent gave pure **2a** in 82% yield (63 mg, 0.16 mmol). A similar deprotonation with (Bu^n)$_3$P=NBu^t gave **2a** in quantitative yield as determined by IR monitoring. With the same reaction conditions, complex **6b** was transformed into **2b** in quantitative yield by IR.

Methylation of 5a To Form 7a. A CH_2Cl_2 solution of complex **3a** (100 mg, 0.27 mmol) was placed in a 100-mL Schlenk flask and stirred under 1 atm of CO at room temperature for 15 min to form an equilibrium mixture of **3a**/**5a**. Solid $[Me_3O]BF_4$ (56 mg, 0.38 mmol) was then added in one portion. The reaction mixture was stirred under 1 atm of CO for 16 h and filtered and concentrated under vacuum to yield a red oil. The product was redissolved in CH_2Cl_2 (3 mL) and precipitated by adding Et_2O (10 mL) to give **7a** (93.8 mg, 19 mmol) as a red microcrystalline solid in 69% yield. Anal. Calcd for $C_{14}H_{14}BF_4Fe_2NO_7$: C, 33.18; H, 2.78. Found: C, 33.31; H, 2.68. IR (CH_2Cl_2): ν_{CO} 2105 (m), 2077 (vs), 2046 (sh), 2034 (s), 1997 (w) cm^{-1}. ^1H NMR ($CDCl_3$): δ 7.83 (d, 1 H, C*H*, J_{HH} = 2.8 Hz), 6.72 (d, 1 H, C*H*, J_{HH} = 2.8 Hz), 4.09 (s, 3 H, OCH_3), 1.33 (s, 9 H, C(CH_3)$_3$). ^{13}C NMR ($CDCl_3$): δ 227.4 (s, Fe*C*{OMe}CH), 205.6, 204.5, 203.3, 202.7 (*C*O), 127.8 (dd, $^1J_{CH}$ = 191.7 Hz, $^2J_{CH}$ = 6.1 Hz, *C*H), 83.6 (dd, $^1J_{CH}$ = 179.4 Hz, $^2J_{CH}$ = 8.5 Hz, *C*H), 66.7 (m, *C*(CH$_3$)$_3$), 63.1 (q, $^1J_{CH}$ = 148.9 Hz, O*C*H$_3$), 33.4 (m, C-(*C*H$_3$)$_3$).

Reaction of 5a with HBF_4 To form 8a and 9a. A solution of complex **3a** (250 mg, 0.66 mmol) in CH_2Cl_2 (75 mL) was placed in a 200-mL Schlenk flask and stirred under 1 atm of CO at room temperature for 15 min to form an equilibrium mixture of **3a**/**5a**. An Et_2O solution of HBF_4 (0.215 mL, 1.60 mmol) was added over 10 min, and the solution was stirred for 1 h and then concentrated under reduced pressure to 5 mL. The product was precipitated by adding Et_2O. The red solid residue was separated from the supernatant, redissolved in CH_2Cl_2, and again precipitated by the addition of Et_2O to yield a mixture of **8a** and **9a** (180 mg; **8a**, 0.31 mmol, 47%; **9a**, 0.05 mmol, 8% by ^1H NMR) as a red microcrystalline solid.

Data for 8a. IR (CH_2Cl_2): ν_{CO} 2106 (m), 2069 (vs), 2035 (s), 1991 (w) cm^{-1}. ^1H NMR ($CDCl_3$): δ 10.17 (br, 1 H, O*H*), 7.37 (d, J_{HH} = 2.7 Hz, 1 H, C*H*), 6.53 (d, J_{HH} = 2.7 Hz, 1 H, C*H*), 1.32 (s, 9 H, C(CH_3)$_3$). ^{13}C NMR ($CDCl_3$): δ 228.4 (s, Fe*C*{OH}CH), 205.8, 204.7, 203.5, 202.8 (*C*O), 126.3 (dd, $^1J_{CH}$ = 190.4 Hz, $^2J_{CH}$ = 7.3 Hz, *C*H), 87.0 (dd, $^1J_{CH}$ = 179.4 Hz, $^2J_{CH}$ = 9.8 Hz, *C*H), 66.1 (m, *C*(CH$_3$)$_3$), 33.4 (m, C(*C*H$_3$)$_3$).

Data for 9a. IR (CH_2Cl_2): ν_{CO} 2102 (m), 2068 (vs), 2035 (s), 2022 (sh), 1990 (w) cm^{-1}. ^1H NMR ($CDCl_3$): δ 7.33 (d, J_{HH} = 2.5 Hz, 1 H, C*H*), 6.19 (d, J_{HH} = 2.5 Hz, 1 H, C*H*), 1.32 (s, 9 H, C(CH_3)$_3$). ^{13}C NMR ($CDCl_3$): δ 234.4 (d, Fe*C*{OBF$_3$}CH), 206.7, 204.2, 202.2 (*C*O), 125.0 (*C*H), 85.1 (*C*H), 65.9 (m, *C*(CH$_3$)$_3$), 33.3 (m, C(*C*H$_3$)$_3$).

Reaction of $Fe_2(\mu\text{-}CMe_2)(CO)_8$ with $Bu_3P{=}NBu^t$ To form $Fe_2(\mu\text{-}CMe_2)(CO)(C\{O\}N(Bu^t)P(Bu^n)_3)$ (11). The complex $Fe_2(\mu\text{-}CMe_2)(CO)_8$ (100 mg, 0.26 mmol) was dissolved in 50 mL of CH_2Cl_2 and cooled to 0 °C in an ice–water bath, and $Bu_3P{=}NBu^t$ (78 mg, 0.29 mmol) was added dropwise to the solution. Over the course of 2 h, the color changed from yellow to red. The solution was concentrated, and the product **11** (150 mg, 0.23 mmol, 88%) was precipitated as a red oil by addition of pentane. IR (THF): ν_{CO} 2021 (w), 1970 (vs), 1926 (vs), 1752 (w) cm^{-1}. ^1H NMR (CD_2Cl_2): δ 2.90 (s, 6 H, μ-CMe$_2$), 2.07, 1.50, 0.97 (Bu^n), 1.35 (s, 9 H, Bu^t). ^{13}C NMR (CD_2Cl_2): δ 231.7 (*C*{O}NBu^t), 173.4 (μ-*C*Me$_2$), 64.5 (μ-C(CH$_3$)$_2$), 23.5 (C(*C*H$_3$)$_3$), 32.1, 24.7, 24.2, 13.6 (Bu^n). ^{31}P NMR (CD_2Cl_2): δ 53.7.

Reaction of $Fe_2(\mu\text{-}CH_2)(CO)_8$ (1) with *tert*-Butylisocyanide. Complex **1** (200 mg, 0.29 mmol) was dissolved in 60 mL of CH_2Cl_2, *tert*-butylisocyanide (48 mg, 0.58 mmol) was added dropwise, and the solution immediately began to darken. After the solution was stirred for 3 h, the solvent was evaporated and the residue extracted with pentane. The residue, after the pentane extraction, was soluble in CH_2Cl_2. IR analysis showed the presence of carbonyl-containing compounds, but these were not identified. The major component of the pentane-soluble portion was $Fe(CO)_4(C{\equiv}NBu^t)$, which was isolated by repeated crystallization from pentane. EIMS: m/z 251 (M^+). IR (pentane): ν_{CO} 2180 (w), 2059 (m), 1986 (m), 1958 (vs). The presence of $Fe(CO)_3(C{\equiv}NBu^t)_2$ in the mixture was inferred by the observation of a parent ion at m/z 306.

Crystal and Molecular Structures of $Fe_2(\mu\text{-}CH{=}CHNPhC\{O\})(CO)_6$ (2b), $Fe_2(\mu\text{-}CH{=}CHNBu^t)(CO)_6$ (3a), $Fe_2(\mu\text{-}C\{O\}CH{=}CHNPh)(CO)_6$ (5b), $[Fe_2(\mu\text{-}CHCH{=}NHBu^t)(CO)_8][CF_3SO_3]$ (6a'), and $[Fe_2(\mu\text{-}C\{OMe\}{=}CHCH{=}NBu^t)(CO)_8][BF_4]$ (7a). Crystallographic data are presented in Tables II and III. All samples were mounted on glass fibers with epoxy cement. Systematic absences in the diffraction data for **2b** suggested either of the orthorhombic space groups $Pbc2_1$ or $Pbcm$. The inability of the proposed structure of **2b** to possess mirror plane symmetry without disorder confined our initial processing to a model containing two independent molecules in the acentric alternative. The correctness of this choice was confirmed by the absence of a mirror plane relationship between the two independent molecules. The monoclinic space group $P2_1/n$ was uniquely determined for **3a**, **5b**, and **6a'**, and the orthorhombic space group $P2_12_12_1$ was uniquely determined for **7a**. No correction for absorption was required (all values for T_{max}/T_{min} <1.2) for any of the data sets.

All structures were solved by direct methods. All non-hydrogen atoms were refined with anisotropic thermal parameters except for C(8') in **2b**, which became nonpositive definite, and all carbon atoms in **3a** due to a low data to parameter ratio. All hydrogen atoms were treated as idealized contributions except for H(*n*), H(9), and H(10) in **6a'**, which were found and isotropically refined. The phenyl rings in **2b** and **5b** were constrained to rigid, planar hexagons (d(CC) = 1.395 Å). Refinement of a multiplicative term (1.14 (9)) for $\Delta f''$ for **2b** indicated that the enantiomorph reported is correct.

An examination of a partial second octant of data for **2b** showed a nearly random variation in the intensities of equivalent reflections. Hence, only a single form of the data was obtained, and this resulted in a very low data to parameter ratio. All tested samples of crystals of **3a** diffracted diffusely. The crystals appeared layered; under crossed polarizers, interference patterns were seen, indicating some offset of layers.

All computations used SHELXTL software (version 5.1) (G. Sheldrick, Nicolet XRD, Madison, WI).

Acknowledgment. We thank the Office of Basic Energy Sciences, Department of Energy, for support of this research and the National Science Foundation for providing funds to support the purchase of the X-ray diffractometer at the university of Delaware.

Supplementary Material Available: For **2b**, **3a**, **5b**, **6a'**, and **7a**, tables of anisotropic thermal parameters, bond lengths and angles, and calculated hydrogen atom positions (19 pages); tables of structure factors for the same compounds (72 pages). Ordering information is given on any current masthead page.

The Peroxide-Dependent μ_2-O Bond Formation of $[Mn^{IV}SALPN(O)]_2$

Erlund J. Larson and Vincent L. Pecoraro*

Contribution from the Department of Chemistry, Willard H. Dow Chemical Laboratories, University of Michigan, Ann Arbor, Michigan 48109-1055. *Received May 29, 1990*

Abstract: A variety of Mn^{III}SALPN complexes as monomeric and dimeric derivatives have been prepared. Acetonitrile solutions of tetragonal complexes such as $[Mn^{III}(SALPN)(CH_3OH)_2]ClO_4$, **1**, are unreactive with hydrogen peroxide unless base is added. In contrast, $[Mn^{III}(SALPN)(AcAc)]$, **2**, $[Mn^{III}(SALPN)(OCH_3)]_2$, **3**, and $Mn^{III}_2(SALPN)_3$, **4**, internally carry an equivalent of base and react rapidly to form the oxidized dimer $[Mn^{IV}(SALPN)(O)]_2$, **5**. The base is required to deprotonate hydrogen peroxide prior to reaction with **1**–**4**. Alkyl peroxides such as *tert*-butyl hydroperoxide also require base for reactivity but appear to follow a different mechanistic pathway consistent with the slow loss of *tert*-butoxide leading to Mn^{V}OSALPN, **19**. The conversion of **2**, **3**, or **4** to **5** has been examined with use of isotopically labeled hydrogen peroxide and ring-substituted ligand derivatives. These data demonstrate that the first intermediate in the reaction is probably a monomeric hydroperoxide adduct $[Mn^{III}(SALPN)(O_2H)]$, **16**. The monomer **16** then reacts with another equivalent of $Mn^{III}(SALPN)(X)$ to form a peroxo-bridged dimer $(SALPN)Mn^{III}(O_2)Mn^{III}(SALPN)$, **17**, which undergoes internal electron transfer forming **5**. This proposed mechanism is consistent with X-ray structural characterization of the precursors $(Mn^{III}(SALPN)(AcAc)$, **2**, $[Mn^{III}(5\text{-Cl-SALPN})(CH_3OH)_2]ClO_4$, **7**, $[Mn^{III}(3,5\text{-diCl-SALPN})(CH_3O)]_2$, **12**, and $Mn^{III}_2(SALPN)_3$, **4**) and product (**5**) complexes in the solid state and ^1H NMR spectra of the Mn(III) species in methylene-d_2 chloride/5% methanol-d_4 at 22 °C. Electrochemistry and isotope labeling experiments show that monomeric compounds such as $[Mn^{IV}(SALPN)(AcAc)]PF_6$, **6**, $Mn^{IV}O(SALPN)$, or $[Mn^{V}(O)SALPN)]ClO_4$ cannot be involved in the hydrogen peroxide-dependent transformation to form **5**. In contrast, intermediates such as **19** are implicated in the *tert*-butyl peroxide oxidations. X-ray parameters for **2**, $C_{22}H_{23}N_2O_4Mn_1$, 434 g/mol, crystal system, monoclinic ($P2_1/c$), a = 8.004 (3) Å, b = 14.035 (8) Å, c = 18.134 (6) Å, β = 83.30 (3)°, V = 2023 (2) Å^3, Z = 4, 2666 data collected with $3° < 2\theta < 45°$, 1624 data with $I > 3\sigma(I)$, R = 0.0503, R_w = 0.0503; **4**, $Mn_2N_7O_6C_{56}H_{53}$, 1029 g/mL, crystal system triclinic ($P\bar{1}$), a = 11.011 (4) Å, b = 14.103 (5) Å, c = 17.174 (7) Å, α = 74.59 (3)°, β = 83.82 (3)°, γ = 82.28 (3)°; V = 2540 (2) Å^3, Z = 2, 6104 data collected with $3° < 2\theta < 45°$, 4416 data with $I > 3\sigma(I)$, R = 0.0475, R_w = 0.0360; **7**, $C_{19}H_{22}N_2O_8MnCl_3$, 566 g/mol, crystal system, monoclinic ($P2_1/c$), a = 10.579 (4) Å, b = 17.451 (11) Å, c = 13.651 (6) Å, β = 112.75 (3)°, V = 2324 (2) Å^3, Z = 4, 2178 data collected with $3° < 2\theta < 45°$, 1693 data with $I > 3\sigma(I)$, R = 0.0524, R_w = 0.0457; **12**, $Mn_2Cl_8N_4O_7C_{37}H_{33}$, 1039 g/mL, crystal system monoclinic ($P2_1/n$), a = 9.213 (5) Å, b = 26.024 (16) Å, c = 17.992 (7) Å, β = 91.87 (4)°, V = 4312 (4) Å^3, Z = 2, 5639 data collected with $3° < 2\theta < 45°$, 3197 data with $I > 3\sigma(I)$, R = 0.0519, R_w = 0.0470.

Introduction

Manganese plays an important role in the metabolism of dioxygen and its reduced forms. Three examples are the dismutation of superoxide to hydrogen peroxide and dioxygen by the Mn superoxide dismutase,[1] the conversion of hydrogen peroxide to dioxygen and water by the Mn catalase,[2] and the four-electron oxidation of two water molecules to form dioxygen by the photosynthetic oxygen-evolving complex.[3] The latter two activities require clusters of manganese atoms, presumably since the reactions that they catalyze are multielectron processes.

In recent years, knowledge of the structural organizations of these multinuclear manganese enzymes has been placed on a more sound footing through EPR, X-ray absorption, and X-ray crystallographic studies. Both the oxygen-evolving complex[4-6] and the Mn catalase[7,8] have EPR spectral signatures indicative of coupled manganese centers. The Mn catalase has been crystallized,[9] and a low-resolution map has been presented which places

(1) (a) Ludwig, M. L.; Pattridge, K. A.; Stallings, W. C. *Metabolism and Enzyme Function*; Academic Press, Inc.: New York, 1986; p 405. (b) Stallings, W. C.; Pattridge, K. A.; Strong, R. K.; Ludwig, M. L. *J. Biol. Chem.* **1985**, *260*, 16424.

(2) (a) Penner-Hahn, J. E. In *Manganese Redox Enzymes*; Pecoraro, V. L., Ed.; Verlag-Chemie: New York, Chapter 2, in press. (b) Kono, Y.; Fridovich, I. *J. Biol. Chem.* **1983**, *258*, 13646. Beyer, W. F., Jr.; Fridovich, I. *Biochemistry* **1985**, *24*, 6460.

(3) (a) Babcock, G. T.; Barry, B. A.; Debus, R. J.; Hoganson, C. W.; Atamain, M.; McIntosh, L.; Sithole, I.; Yocum, C. F. *Biochemistry* **1989**, *28*, 9557. (b) Rutherford, A. W. *Trends Biochem. Sci.* **1989**, *14*, 227. (c) Ghanotakis, D. F.; Yocum, C. F. *Ann. Rev. Pl. Physiol.* **1990**, *41*, 255. (d) Christou, G. *Acc. Chem. Res.* **1989**, *22*, 328. (e) Pecoraro, V. L. *Photochem. Photobiol.* **1988**, *48*, 249. (f) Wieghardt, K. *Angew. Chem., Int. Ed. Engl.* **1990**, *28*, 1153. (g) Govindjee; Coleman, W. J. *Sci. Am.* **1990**, *262*, 50.

(4) Dismukes, G. C.; Siderer, Y. *Proc. Natl. Acad. Sci. U.S.A.* **1981**, *78*, 274.

(5) Hannson, O.; Aasa, R.; Vanngard, T. *Biophys. J.* **1986**, *51*, 825.

(6) (a) de Paula, J. C.; Innes, J. B.; Brudvig, G. W. *Biochemistry* **1985**, *24*, 8114. (b) de Paula, J. C.; Beck, W. F.; Brudvig, G. W. *J. Am. Chem. Soc.* **1986**, *108*, 4002.

(7) Khangulov, S. V.; Barynin, V. V.; Melik-Adamyin, V. R.; Grebenko, A. I.; Voevodskaya, N. V.; Blumenfeld, L. A.; Dobryakov, S. N.; Il'Yasova, V. B. *Bioorg. Khim.* **1986**, *12*, 741.

(8) Fronko, R.; Penner-Hahn, J. E.; Bender, C. *J. Am. Chem. Soc.* **1988**, *111*, 7554.

(9) Barynin, V. V.; Vagin, A. A.; Melik-Adamyan, V. R.; Grebenko, A. I.; Khangulov, S. V.; Popov, A. N.; Andrianova, M. E.; Vainshtein, B. K. *Sov. Phys. Dokl.* **1986**, *31*, 457.

0002-7863/91/1513-3810$02.50/0 © 1991 American Chemical Society